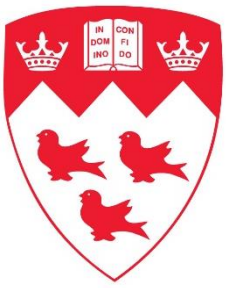

Colorimetric Detection of Bacteria Using Plasmonic-enhanced Nanostructures for Applications in Point-of-Care Settings

Haleema Khan

Master of Engineering

Department of Bioengineering

McGill University

Montreal, Quebec, Canada

July 2022

A thesis submitted to McGill University in partial

fulfillment of the requirements of the degree of

Master of Engineering

Abstract

Infectious diseases driven by bacteria are a major global health concern and one of the leading causes of death worldwide. Reducing the time delay between sample collection and treatment could be lifesaving and would ultimately reduce the burden of bacterial infections on healthcare systems. The current gold standard bacteria diagnostic techniques, including polymerase chain reaction (PCR) and culturing methods, are complex, expensive, and mainly suited to centralized laboratories. Furthermore, the detection of bacteria using these methods takes between 24-72 hours for definitive results, causing delays in treatment plans, and ultimately worsening a patient's health conditions. The challenge is to reduce the cost, complexity, and time of the conventional methods, while maintaining their sensitivity and accuracy in bacteria detection.

Colorimetric assays in combination with surface plasmon resonance can address the long-standing need for rapid detection of bacterial nucleic acids and have gained significant traction in the diagnostics space. Changes in the molecular environment, including DNA amplification, can be readily monitored using color-changing dyes. Moreover, plasmonic surfaces printed on nanostructures can enable high color tunability across the visible spectrum, leading to extraordinary optical sensitivity. This technique typically involves affordable reagents, sensitive optical readout mechanisms, and fast response times, lending itself to a range of clinical applications, particularly in point-of-care (POC) settings.

In this thesis, I present a study on the rapid detection of bacterial DNA using a plasmonic-enhanced colorimetric biosensor. This biosensor integrates a plasmonic color-sensitive platform, loop-mediated isothermal (LAMP) assay, microfluidic channels, and on-chip heating to enable rapid, simple, and sensitive detection of samples. The reaction changes color in the presence of

phenol red due to DNA amplification by the primers, releasing H^+ ions in the process. Enhanced color sensitivity is further achieved by a plasmonic platform consisting of a self-assembled monolayer of aluminum coated nanostructures, coupled with a zinc-oxide back-reflector. We applied our biosensor to detect nucleic acids from *Escherichia coli*, *Pseudomonas aeruginosa,* and Methicillin-resistant *Staphylococcus aureus* – three pathogenic bacteria with high rates of morbidity and mortality. We were able to detect bacterial DNA as early as 7 min for high concentrations and up to 15 min for low concentrations. The limit of detection was as low as 0.2 ng/µL, which is a highly sensitive response. Importantly, our biosensor has also demonstrated the possibility for translation in POC settings. This study validates our biosensor, as a robust avenue for bacterial DNA detection in a time-sensitive manner, shedding light on the value of plasmonic-assisted color sensing for diagnostics.

Overall, plasmonic materials can be employed to reduce the detection window of biosensors for clinical applications and POC settings. An important consideration in this area is the quantification of colorimetric signals for integration with smart gadgets, which would ultimately enable portability and user-friendliness. Affordable and compact imaging of colorimetric readouts is also crucial in order to facilitate applications at the POC. Future work should consider these factors to facilitate rapid diagnostic and therapeutic protocols to control the spread and burden of infectious diseases driven by bacteria.

Keywords: bacteria detection, colorimetry, plasmonic, nanostructures, biosensor

Résumé

Les maladies infectieuses causées par des bactéries constituent un problème de santé mondial majeur et l'une des principales causes de décès dans le monde. Réduire le délai entre le prélèvement d'un échantillon et le traitement pourrait sauver des vies et, à terme, réduire la charge des infections bactériennes sur les systèmes de santé. Les techniques actuelles de diagnostic bactérien de référence, notamment la réaction en chaîne par polymérase (PCR) et les méthodes de culture, sont complexes, coûteuses et principalement adaptées aux laboratoires centralisés. En outre, la détection des bactéries à l'aide de ces méthodes nécessite entre 24 et 72 heures pour obtenir des résultats définitifs, ce qui retarde les plans de traitement et, en fin de compte, aggrave l'état de santé des patients. Le défi consiste à réduire le coût, la complexité et le temps des méthodes conventionnelles, tout en maintenant leur sensibilité et leur précision dans la détection des bactéries.

Les tests colorimétriques combinés à la résonance plasmonique de surface peuvent répondre au besoin de longue date de détection rapide des acides nucléiques bactériens et ont gagné en popularité dans le domaine du diagnostic. Les changements dans l'environnement moléculaire, y compris l'amplification de l'ADN, peuvent être facilement surveillés à l'aide de colorants changeants. De plus, les surfaces plasmoniques imprimées sur des nanostructures peuvent permettre un réglage élevé de la couleur dans le spectre visible, ce qui entraîne une sensibilité optique extraordinaire. Cette technique implique généralement des réactifs abordables, des mécanismes de lecture optique sensibles et des temps de réponse rapides, ce qui se prête à une série d'applications cliniques, en particulier dans les points de soins (POC).

Dans cette thèse, je présente une étude sur la détection rapide de l'ADN bactérien à l'aide d'un biocapteur colorimétrique renforcé par des plasmons. Ce biocapteur intègre une plateforme plasmonique sensible à la couleur, un test isotherme à médiation en boucle (LAMP), des canaux microfluidiques et un chauffage sur puce pour permettre une détection rapide, simple et sensible des échantillons. La réaction change de couleur en présence de rouge de phénol en raison de l'amplification de l'ADN par les amorces, libérant des ions H+ au cours du processus. Une sensibilité accrue à la couleur est obtenue grâce à une plateforme plasmonique constituée d'une monocouche auto-assemblée de nanostructures recouvertes d'aluminium, couplée à un rétro-réflecteur en oxyde de zinc. Nous avons appliqué notre biocapteur pour détecter les acides nucléiques d'Escherichia coli, de Pseudomonas aeruginosa et de Staphylococcus aureus résistant à la méthicilline, trois bactéries pathogènes présentant des taux élevés de morbidité et de mortalité. Nous avons pu détecter l'ADN bactérien dès 7 minutes pour les fortes concentrations et jusqu'à 15 minutes pour les faibles concentrations. La limite de détection minimale était de 0,2 ng/µL, ce qui constitue une réponse très sensible. Un point particulièrement significatif est que notre biocapteur a également démontré la possibilité d'être appliqué dans des environnements POC. Cette étude valide notre biocapteur en tant que moyen robuste de détection de l'ADN bactérien dans un laps de temps très court, et met en lumière la valeur de la détection colorée assistée par les plasmons pour le diagnostic.

Dans l'ensemble, les matériaux plasmoniques peuvent être utilisés pour réduire la fenêtre de détection des biocapteurs pour les applications cliniques et les environnements POC. Une considération importante dans ce domaine est la quantification des signaux colorimétriques pour l'intégration avec des gadgets intelligents, ce qui permettrait finalement la portabilité et la facilité d’usage. L'imagerie abordable et compacte des relevés colorimétriques est également cruciale pour

faciliter les applications au centre de soins. Les travaux futurs devraient tenir compte de ces facteurs pour faciliter les protocoles de diagnostic et de traitement rapides afin de contrôler la propagation et la charge des maladies infectieuses causées par les bactéries.

Mots clés: détection des bactéries, colorimétrie, plasmonique, nanostructures, biocapteur

Contribution of Authors

Chapter 4 of this thesis is a prepared manuscript to be submitted with the title: “Ultra-rapid Detection of Bacterial DNA Using Plasmonic-enhanced Colorimetric Biosensor” with Haleema Khan as the first author. The fabrication processes were performed at the McGill Nanotools-Microfab, primarily by Tamer AbdElFateh. The DNA extraction of Methicillin-resistant *S. aureus* and *P. aeruginosa* was conducted at the Dao Lab in the Meakins-Christie Laboratories at the McGill University Health Center Research Institute (MUHC). The scanning electron characterization was performed at the Facility for Electron Microscopy Research (FEMR) at McGill University. Tamer AbdElFateh contributed significantly to the experimental design and planning of the fourth chapter of this thesis. Mahsa Jalali provided guidance on the statistical analysis and assisted with resazurin experiments. Olivia Jeanne extracted the data from microscopy images using deep learning. Carolina del Real Mata assisted with resazurin experiments, the fabrication of the colorimetric platforms, and with optical UV-visible studies. Dr. Roozbeh Siavash Moakhar assisted with electrochemical studies. Dr. Seyed Vahid Hamidi and Dr. Sara Mahshid provided guidance and valuable insight on the discussion of the results. All other material is original, unpublished work by the author, Haleema Khan.

Acknowledgements

None of this work would have been possible without the mentorship and guidance of my supervisor, Dr. Sara Mahshid, who faithfully took on a young, determined Neuroscience undergrad. Dr. Sara's ambition and high standards made me a better scientist. Her passion for science has infused every inch of our lab, and she inspires me to stay curious. Simply put, thank you Dr. Sara.

A thank you goes to all of the faculty and staff at McGill and UQAM for their constant willingness to help. Specifically, thank you to Pina Sorrini, Sabrina Teoli, and Xavier Elisseeff, who have always helped me troubleshoot and find answers to my questions.

I am incredibly grateful to everyone at the Mahshid Lab for helping me stay positive and motivated throughout my Master's degree. Tamer: you are an incredible scientist and even better friend; you have always found a way to make long days of imaging in the lab enjoyable for everyone and I will miss working with you. Sri and Olivia: I could not have navigated the obstacles in my Master's alone. You never failed to put my stresses at ease and keep me balanced. Roozbeh and Mahsa: you are both brilliant scientists, and two gems that the lab is fortunate to have. Carolina: you always found a way to bring positivity and light into long working days, I will miss discussing tennis with you. Vahid: thank you for happily answering my biology-related questions and for serving as a compass in drafting my manuscript and thesis. Hamed: you are an amazing desk-mate and person to work with, I know you will accomplish incredible things in your PhD. Imman and Arash: I have been fortunate to get to work with you and I am excited to follow your contributions to the field.

I would also like to thank my mentors at the University of Toronto, my colleagues in the Schulich Leaders Network, and my friends from Westlane, U of T, and McGill. You have always believed in me and made me feel like I was capable of anything. Briefly, I am grateful for a village of incredible people in my life.

To Aleem: you have been my greatest supporter during my Master's degree and words cannot express how much you uplifted me during the hardest days. You are truly a beacon of light.

Finally, my Mama and Papa have been unwavering in their support throughout all my dreams and ambitions. They have made tremendous sacrifices to open possibilities for my brother and I, and I will forever be indebted to them. I am so lucky to have a family that is full of eternal love and support. To Mama, Papa, and Shameer: you are the reason that I have stayed motivated and happy in my career, and I hope I have made you proud.

Table of Contents

List of Figures and Tables

List of Abbreviations

POC	Point of care or point-of-care
WHO	World Health Organization
LAMP	Loop-mediated isothermal amplification
PCR	Polymerase chain reaction
ELISA	Enzyme-linked immunosorbent assay
DNA	Deoxyribonucleic acid
RNA	Ribonucleic acid
LOD	Limit of Detection
E. coli	*Escherichia coli*
S. aureus	*Staphylococcus aureus*
P. aeruginosa	*Pseudomonas aeruginosa*
CFU	Colony-forming unit
SPR	Surface plasmon resonance
SAM	Self-assembled monolayer
Al	Aluminum
ZnO	Zinc-oxide
PDMS	Polydimethylsiloxane
TMB	3,3',5,5'-Tetramethylbenzidine
RPM	Revolutions per minute
HRP	Horseradish peroxidase

1 Introduction

This thesis discusses the detection of pathogenic bacteria for point-of-care applications. Although there has been extensive research on biosensors for the detection of bacteria, as reported in Chapter 2, the review identifies a need for a biosensor with a faster response time while detecting with high sensitivity and ensuring accuracy in sample detection.

Plasmonic nanostructures have shown promise in filling this gap by facilitating extraordinary optical sensitivity. This combined with colorimetric nucleic acid amplification techniques such as LAMP, can enable the detection of sufficiently low sample concentrations. This principle is at the centre of our work in Chapter 4. Chapter 4 presents a prepared manuscript on a novel plasmonic-enhanced biosensor for the colorimetric detection of bacterial DNA.

Objectives

The main objectives of our research were: 1) to investigate the most optimal color-changing dye for our LAMP assay, 2) to study the plasmonic effect of our biosensor through electrochemistry studies, 3) to validate the specificity of each primer set in an off-chip LAMP assay and in the biosensor, 4) to determine the sensitivity of our biosensor in detecting samples in the physiological range, and 5) to test simulated biological samples.

Hypothesis

We hypothesized that our novel, plasmonic-enhanced colorimetric biosensor would lead to a faster response time compared to standard approaches due to the application of plasmonic nanostructures.

2 Literature Review: Colorimetric Detection of Bacteria at the Point-of-Care

2.1 Background

Bacteria are pervasive. While most bacteria are critical in maintaining a well-balanced environment, a small percentage can cause serious infections and diseases which pose a grave danger to public health (1). Bacterial infections can spread through various modes of transmission including contact, airborne droplets, or living vectors (2–4). Moreover, bacterial pathogens can manifest as diseases in multiple ways. For example, *Staphylococcus aureus* is typically prevalent in skin or mucus membranes and triggers soft tissue infections (5). In addition, bacterial infections can sometimes spread to critical organs of the body and induce severe infections. Notable cases are lower respiratory tract infections and diarrhea, which are among the top 10 causes of mortality worldwide (6,7). In 2019 alone, 1.27 million lives were taken globally by bacterial infections – more deaths than HIV/AIDS or Malaria – where the largest impact was in low-resource communities (8).

Several factors are at play in the predicament of the burden of bacterial infections on healthcare systems, among which include significant delays in diagnosis and therapeutic measures (9), high cost of diagnostic instruments (10), and the necessity for trained personnel to perform tests (11). Moreover, the emergence of antibiotic-resistant strains has aggravated the issue, as new resistance mechanisms are spreading widely, threatening our ability to respond to common infectious diseases. As a result, the World Health Organization (WHO) has identified antibiotic resistance as one of the largest global threats of the 21st century, with a predicted mortality rate of 10 million annually, by 2050 (12). It is without question that preventative measures such as

eliminating the source of the infection and slowing transmission can have drastic effects on survival rates.

Surveillance measures have been implemented in the US and EU to gather epidemiological data, monitor research efforts, and acquire information on government networks to provide accurate and timely information regarding disease trends (13). This has enabled healthcare networks and first responders to identify disease hotspots and take action accordingly. Despite these efforts, there still remain surveillance gaps in many parts across the world (14). This, in large part, is due to the inability to correctly detect and identify pathogenic bacteria in accordance with high sensitivity, specificity, low-cost, and fast response times (15). This highlights the importance of rapid and accurate identification of bacterial pathogens at the onset of infections, in order to control the spread and burden of infectious diseases driven by bacteria.

2.2 Standard Methods for Bacteria Detection

Conventional routes for bacteria detection encompass culture-based and microscopy techniques, molecular techniques, and immunoassays. Of these, culture based techniques are one of the oldest methods for bacterial detection used in both diagnosis and susceptibility testing (16–18). While culture techniques provide an economical method for bacteria detection they suffer from being laborious and for extended periods of time up to 72 h for diagnostic results (19).

In contrast, PCR, LAMP, and ELISA provide results within a few hours, making them more favorable for on-site applications (20, 21). PCR is currently the gold standard technique for the detection of nucleic acids *in vitro* due to its rapid amplification of target DNA sequences, resulting in fast and high-throughput detection (22, 23). This has led to its prominence as a clinical tool in the diagnosis of bacterial and viral pathogens (24–26). Similarly, isothermal amplification

techniques such as loop-mediated isothermal amplification (LAMP), are valuable for rapid detection of nucleic acids (27). Constant temperatures of LAMP provide a less complicated alternative to PCR, making them suitable for on-site applications (28). Immunoassays, including enzyme-linked immunosorbent assay (ELISA), are another standard detection method which employ an antibody, antigen, or an aptamer to target the compound of interest (29). ELISA tests for the presence of a specific antigen or ligand using an antibody, and an enzyme reacting with its substrate for target molecule detection (30). Despite the high sensitivity, specificity, and efficacy of PCR, LAMP, and ELISA for pathogen detection (31,32), these techniques require trained technicians, specific machinery, and expensive preparation of samples in laboratory settings making them less favored options for smaller labs and resource-limited settings (33–35).

Standard diagnostic techniques underscore the need for translation in resource-limited or point-of-care (POC) settings. To facilitate this, these techniques need to incorporate scaled-down sizes, affordable reagents, and user-friendly interfaces, while adhering to high standards of sensitivity and accuracy. Ultimately, this would make diagnosis of bacterial infections more accessible for individuals in communities that are distant from centralized laboratories, which is of utmost importance as these groups are often most at risk.

2.3 Point-of-Care Diagnostics

Point-of-care (POC) diagnostics has been a priority in research work in the past decade in an effort to equip at-risk communities to effectively combat infectious diseases and ultimately make healthcare more accessible (36). Typical assays can be integrated in POC devices in order to maintain high standards of sensitivity, specificity, and accuracy of tests while ensuring aspects such as ease of operation, fast response times, and simple methods of detection (37). Typically,

this includes tests that do not require the use of trained laboratory technicians or large facilities to provide results (38). Moreover, POC tests can be applied in clinical settings, at home, or in the field to test samples with response times on the order of seconds to hours (39). The tests involve straightforward protocols, and the readout can be as simple as detecting a particular color on a strip of paper (40).

Microfluidics have been paramount in designing POC devices over the past decade. Microfluidics can be incorporated into POC devices to control the sample flow rate, reagent mixing, and the filtration of analytes on a sub-milliliter scale (41). The small sample and reaction volumes enable high-throughput detection and fast response times, which are particularly important for detecting infections on-site (41). Another important feature of microfluidics is that they can integrate sample processing, extraction, and analysis onto a single device, which lends themselves to applications in POC settings (42). Simply put, portability and precision are two important advantages of microfluidics that make them ideal for POC detection (43).

Overall POC diagnostics are necessary to make disease tracking more manageable, accessible, and timely for individuals in remote, isolated, and low-resource settings. From the abundance of positive aspects of POC diagnostics, three qualities underline their key advantages over standard diagnostic techniques, namely: time, patient-accessibility, and cost. In comparison to standard diagnostic tests, samples need not be transported to centralized laboratory facilities or wait for the skilled handling of trained laboratory technicians (44). Instead, results can be received on-site, and therapeutic measures can be determined rapidly, avoiding worsening patient conditions or spreading the infection to other individuals (45). Accessibility for patients is a huge advantage as patients can assume control and management of their own conditions through user-friendly biosensors, evading constant hospital visits, travel costs, and time away from work. This

is best exemplified by the advent of glucose meters (46), at-home pregnancy tests (47), and COVID-19 rapid antigen tests (48). POC diagnostic devices often cost less than those in conventional laboratories. For instance, many POC devices often cost under $2 USD (37) which is a stark contrast to standard tests which can range between $10, 000 - $20, 000 per patient (49). While, POC diagnostics provide many key advantages, it is important to maintain accuracy, sensitivity, and avoidance of false-positives and false-negatives in order to truly substitute them for standard laboratory tests.

2.4 Plasmonic-enhanced Colorimetric Detection

Standard assays and readout techniques can be employed in POC tests, with one of the most prominent readout techniques being colorimetric detection. Colorimetric methods encompass fluorescent or color-changing dyes that lead to variations in signal intensity when exposed to changes in local reaction conditions (50). Examples of color-changing agents include hydroxynaphthol blue (51), phenol red (52), and malachite green (53). These can change color in response to changes in pH or due to the release of chemical agents such as Mg^{2+} (54), allowing one to monitor the progression of a biochemical reaction. Colorimetric detection is attractive because target analytes can be detected rapidly, easily, and with high specificity based on the color change of the reaction (55). Moreover, colorimetric detection enables the sensing of both positive and negative samples (56). Despite this, some limitations of colorimetric detection are the optical sensitivity of the reaction and large volume required which in turn can inflate the cost of a single test.

To overcome the limitations of colorimetric detection methods, plasmonic materials printed on geometric nanostructures have been applied in biosensing to enable high optical

sensitivity of reactions while using low volumes of samples (57). Plasmonic surfaces such as gold, silver, and aluminum can enable high color tunability when printed on nanostructures such as nanorods (56), nanodisks (58), and nanocubes (59). These metallic nanostructures essentially support surface plasmons which are electromagnetic excitations that are coupled with free electrons in a conductive medium (60). The free electrons in the metallic nanostructure will oscillate due to the presence of an external electromagnetic field, such as incident light, in a phenomenon known as surface plasmon resonance (SPR) (61). This leads to resonance at unique wavelengths of light, generating distinctive colors across the visible spectrum, and leading to a highly sensitive optical readout (61). When fabricated in lattices, metallic nanostructures can be integrated in biosensors to tune their optical properties by combining with colorimetric assays. Plasmonic nanostructures have been integrated into biosensors for bacteria detection widely, some of which are reported extensively in section 2.5. Figure 1 depicts a schematic of plasmonic-enhanced colorimetric diagnosis of bacteria, in comparison to standard techniques.

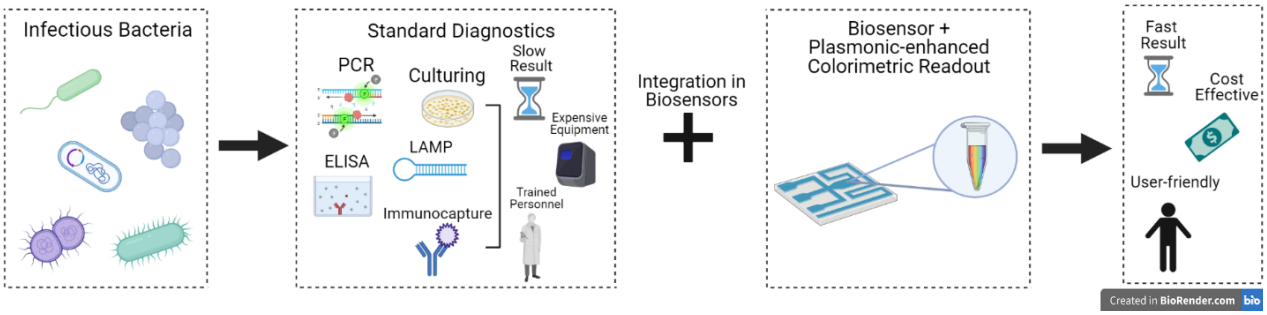

Figure 1: Comparison schematic of standard bacteria diagnostic techniques and plasmonic-enhanced colorimetric detection. Created with BioRender.com.

2.5 Reported Biosensors for Colorimetric Bacteria Detection

2.5.1 Colorimetric PCR-based Detection of Bacteria

Some biosensors have successfully integrated colorimetric PCR assays in scaled-down sizes to detect nucleic acids at the POC. The standard PCR assay encompasses several components as follows: it relies on a series of steps including DNA denaturation, annealing, and extension, by using primers, DNA polymerase, nucleotides, specific ions, and the DNA template (22). The PCR target is amplified by a thermostable DNA polymerase enzyme in the presence of primers and nucleotides through multiple heating and cooling cycles (22). This leads to the amplification of the DNA copy to a billion copies within 3-4 hours (62). One of the main advantages of PCR is that it provides rapid and high-throughput detection and quantification of target DNA sequences (23). Particularly, PCR is notable for its high sensitivity and specificity for pathogens compared to conventional techniques like ELISA (31,32). Additionally, in cases where timely intervention for infectious diseases is required, multi-step culture techniques are not ideal, so PCR is the preferred method (63). However, the phenotypic and biochemical features must be confirmed for bacterial samples after PCR amplification (33). One of the problems with PCR is that it requires trained technicians and specific machinery (33). The cost of reagents (CAD $8-$40) and equipment (CAD $15000) for testing/analyzing specific samples is also high, making PCR suited for centralized laboratories and trained researchers (34).

Integrating PCR into microfluidic platforms brings advantages due to the use of small sample volumes, enabling ‘sample-to-results’ in real time, while reducing costs (64). Recently developed colorimetric PCR-coupled microfluidic platforms for bacteria detection integrating processes from sample preparation to analysis are listed in Table 1. A good example of this is a recent work from Fang et al. (65) which reported a microfluidic-integrated platform for the detection of sepsis induced bacteria. The PCR products were detected by the fluorescent analysis

of the TaqMan amplicon probe. They reported a good sensitivity of 5 CFU/ml which showed minimum interference with blood cellular material facilitated by an enhanced filtration system.

2.5.2 Colorimetric LAMP-based Detection of Bacteria

The advent of isothermal amplification techniques for the molecular detection of pathogenic DNA, provide a less complicated alternative to PCR, making them more suitable for integration into POC biosensors (66). Loop-mediated isothermal amplification (LAMP) is most widely researched among these isothermal techniques for pathogen detection in microfluidic platforms (67–69). The main factors contributing to this are: 1) the requirement of constant temperatures for the denaturation and amplification steps compared to conventional PCR assays, thereby reducing the complexity of components and set-ups, making it more adaptable to POC settings (67); 2) higher specificity and sensitivity compared to conventional techniques (70); and 3) stability against some amplification inhibitors (71). Biosensors integrated with LAMP assays for pathogenic nucleic acid detection have demonstrated POC capabilities in previous works (67,72). The reduced reagent volumes compared to laboratory techniques make them beneficial for use in resource-limited settings, facilitating multiplexed detection assays and reducing assay costs (73,74).

Previously, Azizi et al. (75) reported an application of droplet microfluidics in optimizing the LAMP-based detection of *Salmonella typhimurium.* The microfluidic platform was employed to encapsulate the bacterial RNA and LAMP cocktail in microdroplets resulting from water-in-oil emulsions, essentially creating microdroplet reactors for the amplification to proceed. The amplification reaction and thus the presence of bacterial RNA in cultured samples and contaminated milk samples, was confirmed by the green fluorescence of SYBR dye in positive

samples (75). A mathematical model was also proposed to evaluate the number of droplets required during screening to detect a positive microdroplet; this sped up the process of evaluating detection limits. This approach also resulted in high specificity against other bacterial pathogens. A detection limit of 5000 CFU/ml in spiked solutions for cultured samples was reported. However, the demonstration to some extent lacks applicability at POC, owing to the requirement of fluorescent imaging, the laboratory setup for incubation and amplification, and an RNA extraction step off-chip.

In another work, Seok et al. (76) developed a paper-based fluidic device for the diagnosis of three types of bacterial meningitis DNA, which include *Streptococcus agalactiae*, *Streptococcus pneumonia* and *Staphylococcus aureus* in ~60 min. The device encompassed three fluidic layers, namely, a reaction pad, fluidic channel pad, and transfer pad. These layers were stacked up in the order mentioned, with a sample injection hole in the center. The sample entering from this hole wetted the reaction pad through the fluidic layer. This system used dried LAMP reagents immobilized on the reaction pad which were activated upon interaction with the wet sample. The amplification and thus the amount of bacterial nuclear material was quantified by monitoring the fluorescence of hydroxynaphthol blue whose real time fluorescence activity reduced with the progression of amplification. The device reported a good sensitivity of 4.1×10^2 copies of genomic DNA for *Streptococcus pneumonia* which is better than their previously reported traditional LAMP assay (77) and the specificity of the assay was carried out with multiple other pathogenic DNA, observing no cross-reactivity. The device also showed a proof-of-concept for DNA extracted from clinical bacterial meningitis cultured in the laboratory.

Another work from Seo et al. (78) demonstrated a centrifugal microfluidic platform integrated with LAMP for the detection of foodborne pathogens. Herein the authors designed a

circular microdevice consisting of 24 sample chambers, aliquoting chambers, and amplification reaction chambers. The reaction chambers contained air dried LAMP primer sets while the other components of the LAMP cocktail were loaded with bacterial cells into the sample chambers. Colorimetric detection was mediated by the change of Eriochrome Black T from purple to sky blue for positive samples. The device also exhibited high specificity, with no reports of false positives. Interestingly, the device achieved a lower limit of detection at the 100-cell level compared to the 500-copy level when extracted pathogen DNA was used as the input sample. Overall, this research is one of the first works demonstrating on-chip lysis capabilities through LAMP with bacterial cells as the input sample. This work demonstrated little to no interference of cellular debris in the LAMP reaction, further bolstering the robustness of the LAMP cocktail and proving the applicability of direct-LAMP in microfluidic systems.

Multiplex detection of bacteria is important for applicability in low-resource settings, in connection to this, Zhang et al. (79) reported a centrifugal-based microfluidic platform for LAMP-based detection of six types of bacterial pathogens. The colorimetric change was mediated by calcein which produced a fluorescent signal as the LAMP reaction proceeded, enabling detection by the naked eye under a hand-held UV light. The device consisted of four compartments, one each for the following process: 1) the removal of contaminants using zeolite, 2) addition of the primer mix, 3) mixing of LAMP cocktail, and 4) for the LAMP reaction and colorimetric detection. The systematic flow between the compartments was controlled by the RPM of the centrifugal device. Although the device consolidates the features of sample purification, amplification, and detection onto a single platform, it requires a separate off-chip bacteria cell lysis step. Overall, the device stands out for the inexpensive setup and potential for POC applications.

In addition to these reported works, new techniques like droplet-based digital LAMP and digital PCR techniques may offer enhanced sensitivity (80). A recent work by Ma et al. (81) demonstrated a microdroplet based digital LAMP platform for the diagnosis of vancomycin-resistant *Enterococcus* (VRE) bacteria (Table 1). This is the first work demonstrating the application of emulsion microdroplets for digital LAMP diagnosis of pathogens. The fluorescence of calcein dye was quantified to evaluate the concentration of pathogenic DNA present. Hence the limit of detection of the platform was deduced to be 1 copy of DNA or 50 copies/µl, which is superior compared to other microfluidic platforms (82). This work motivated further exploration of these digital nucleic acid amplification platforms, as they confine reactions to micro-volumes resulting in a low signal-to-noise ratio and enhanced detection even at low-nucleic acid concentrations (83). Several works have been reported in the past 5-6 years on bacterial nucleic acid detection, some of which are discussed above, the core idea being the integration of colorimetric assays onto microfluidic platforms. The recent works revolving around this idea are reviewed in Table 1.

2.5.3 Colorimetric Immunoassay-based Detection of Bacteria

Perhaps one of the most widely researched techniques is the immunoassay for bacteria detection. There are various types of ELISA techniques (called direct ELISA, indirect ELISA, sandwich ELISA, and competitive ELISA) based on the antigen-antibody combination. ELISA detection works by utilizing an antigen which is bound to a solid phase consisting of tubes and microplates made of rigid polystyrene, polyvinyl, and polypropylene (84). Various enzymes can be employed in ELISA including beta galactosidase, beta lactamase, glucose oxidase, peroxidase, and alkaline phosphatase (85,86). The enzyme-substrate reaction is usually completed within 30-60 min and read on a spectrophotometer (35). ELISA has several advantages including high

sensitivity and specificity, and high efficacy. However, disadvantages including the labor intensive and expensive preparation of antibodies, sophisticated techniques, and the possibility of false positives and negatives, make ELISA unfavorable for smaller labs and resource-limited settings (35). Another common immune-based technique is immunocapture, which uses antibodies to capture the antigen of interest. Immunocapture is typically combined with other techniques such as PCR for detection of the analyte of interest. An example of immunocapture-based detection includes immunoblot strips which can be used to quickly diagnose antigens, yet can suffer from low specificity and sensitivity (87). Efforts have been made in recent years in order to incorporate ELISA and immunocapture techniques in biosensors for applications in POC settings.

To adapt their colorimetric device to low-resource settings, Wu et al. (88) reported an electromagnetically driven dual aptamer paper microfluidic assay for the detection of *Acinetobacter baumannii (AB)*. The central idea was to employ two aptamers, wherein the captured antibody was in an immobilized phase for bacterial contaminants to attach to and the biotin labelled detection antibody would form a sandwich conjugate, which, upon the addition of HRP-streptavidin conjugate turns blue in the presence of a TMB substrate. The set-up achieved good specificity and reported a limit of detection of 450 CFU which is far better than other similar paper-based assays, but lower than other techniques reported for the same bacterial pathogen detection.

Zheng et al. (89) demonstrated a magnetic separation based immunocapture assay for the detection of *E. coli O157:H7*. The assay workflow involved three main components: 1) an inlet port followed by a serpentine mixing channel for mixing the *E. coli* sample with capture Abs conjugated magnetic nanoparticles (MNPs) and detection Abs and catalysate conjugated polystyrene microspheres (PSs), 2) a separation chamber for magnetically separating the sandwich complex the bacteria forms with MNPs and PSs, and 3) an inlet port to introduce a horseradish

peroxide mixture followed by the introduction of gold nanoparticles and crosslinking agents. This was coupled with a detection chamber for analyzing the color change of gold nanoparticles. The color in the detection chamber changed from blue to red upon aggregation of gold nanoparticles. The device demonstrated good specificity and a relatively fast response time of 60 min.

Overall, nucleic acid and immunoassay based colorimetric biosensors have an average assay time of ~90 min, which is a significant improvement from traditional techniques including PCR which typically takes several hours to days (90) and ELISA which takes 6-7 h (91). The devices moreover achieved comparable, if not better, sensitivity and detection limits than traditional off-chip techniques, with the lowest being ~3 CFU/µl. Whereas, traditional PCR typically has a sensitivity of $10\text{-}10^2$ CFU/mL (90). This rapidity in detection and high sensitivity can be attributed to requiring low sample volumes, high reaction rates at confined volumes in microfluidics, and reliable colorimetric detection agents that are sensitive to reaction products. Bacterial infections in general are highly communicable as the common mode of transmission is contaminated water and food (92). There are devices that are commercialized mainly for bacteria detection in water, air, and food material (93) and going forward emphasis will be put on commercializing tests for antibiotic resistant bacterial strains in clinical samples. Other works pertaining to nucleic acid and immunoassay integrated microfluidics are reported extensively in Table 1.

Table 1: Summary of colorimetric biosensors for diagnosis of bacteria pathogens.

Pathogen	Detection mechanism	Sample processed	Limit of detection (LOD)	Specificity	Analysis time	Reference
PCR						
Streptococcus mutans, methicillin-susceptible *Staphylococcus aureus* (MSSA) and methicillin-resistant *S. aureus* (MRSA) genomic DNA	Fluorophore detection	Saliva	8–12 copies of MSSA gDNA	None	2 h	(64)

Escherichia coli, *Staphylococcus epidermidis*, and *Staphylococcus saprophyticus*	Fluorescence analysis	Blood	5 CFU/ml	None	4 h	(65)
LAMP						
P. hauseri, *Salmonella* and *E. coli*	Fluorescent intensity analysis via calcein	In vitro spiked samples for analysis.	1.6 copy number for *salmonella*	None	110 min	(94)
Salmonella typhimurium	Turbidity analysis of white precipitate	Spiked samples and Proof of concept established with meat samples	14 CFU/ml	*Listeria monocytogenes*, *E. coli* O157:H7 and *Vibrio parahaemolyticus.*	90 min	(95)
Simultaneous detection of *Staphylococcus aureus*, *Salmonella*, Shigella, enterotoxigenic Escherichia coli, and Pseudomonas aeruginosa	Visual color change of LAMP mixture purchased commercially	Spiked samples and contaminated water	Sau and Sal were both 10^2 copies/µL, whereas the LODs for Sty, Pae, and Eco were as low as 10^1 copies/µL	None	70 min	(96)
E. coli O157:H7, *Salmonella typhimurium*, and *Vibrio parahaemolyticus.*	Color change mediated by eriochrome black (UV-visible detection)	In vitro spiked sample	100 cells/ml	None	60 min	(97)
Salmonella spp., *Staphylococcus aureus*, and *Escherichia c*oli O157:H7	Fuchsin mediated color change	Bacteria spiked milk and juice samples	3.0×10^1 CFU/sample of *Salmonella spp*. and *Escherichia coli* O157:H7 and 3.0×10^2 CFU/sample of *Staphylococcus aureus*	None	75 min	(98)
Salmonella typhimurium	Fluorescence analysis of SYBR green dye	*Salmonella typhimurium* in milk samples	5000 CFU/mL in the sample or 25 RNA template/25 µL LAMP reaction cocktail	LAMP reaction with *S. flexneri* (Gram-negative) and *S. aureus* (Gram-positive).	Not reported	(75)
Multiplex detection of *P. aeruginosa*, *S. typhimurium*, *V. parahaemolyticus*, *V. vulnificus*, *S. iniae*, or *V. alginolyticus*	Fluorescent intensity analysis elicited by calcein under handheld UV light	In vitro bacteria spiked samples.	2×10^2 cells per µL	None	Not reported	(79)
Multiplex detection of *Salmonella spp*, *E. coli* and *Vibrio cholera*	Calcein based visual detection from yellow to green on a centrifugal based chip	Bacteria spiked chicken meat samples	3×10^{-5} ng/µL of bacterial DNA.	Same set of primers for different bacteria *Salmonella*, *S. aureus, S. sonnei*, *L. monocytogenes, Yersinia spp., A. baumannii, E. coli and Vibrio cholerae*	65 min	(99)
Food borne pathogens in general, *Staphylococcus aureus* (SA) and *Vibrio parahaemolyticus* (VP)	Mixed-dye containing hydroxyl naphthol blue (HNB) and SYBR Green I, which elicits green for positive samples and orange-red for negative samples	Bacteria spiked shrimp samples	21.5 and 20.9 copies μL^{-1} for SA and VP plasmid templates respectively	Specificity showed with using SA primer for VP plasmid template and vice versa	Not reported	(100)
Vancomycin-resistant	Florescent analysis of calcein dye	DNA spiked in vitro samples	1 copy of DNA or 50 copies/µl	Not reported	~40 min	(101)

Enterococcus (VRE) bacteria						
E. coli, A. baumannii , SA and MRSA	Fluorescence detection of calcein	Clinical human joint fluidic samples	5fg-50pg for four different bacterial primer sets	Single primer set to monitor LAMP progression of target and non-target bacterial genes.	~65 min	(102)
Bacterial meningitis DNA, that include *Streptococcus agalactiae, Streptococcus pneumoniae, Staphylococcus aureus*	Fluorescence analysis of HNB. High fluorescence for negative samples and low florescence for positive samples.	Clinical patient DNA samples extracted from culture bacterial meningitis	4.1×10^2 copies of genomic DNA for *Streptococcus pneumoniae*	Reported no cross-reactivity for multiple pathogenic DNA.	~60 min	(76)
Escherichia coli, Proteus hauseri, Vibrio parahaemolyticus, and Salmonella subsp. Enterica	Calcein elicited florescence analysis.	Spiked human serum samples	3 copies/µl	None	120 min	(103)
Escherichia coli O157:H7, *Salmonella typhimurium* and *Vibrio parahaemolyticus*	Eriochrome Black T (EBT)-mediated colorimetric change from purple to sky blue.	Cultured bacterial cells and extracted genomic DNA.	500 copies when extracted DNA is sample input and 100 copies when bacterial cells are directly used as sample input.	None	60 min	(78)
Bacterial meningitis- *N. meningitidis, S. pneumoniae*, and *Haemophilus influenzae type b (Hib)*	Calcein mediated detection by naked eye under UV light on a PDMS/paper hybrid microfluidic device.	Spiked samples	LODs of *N. meningitidis, S. pneumoniae* and Hib were 3 copies, 6 copies and 5 copies per LAMP zone for 2 µl of sample solution.	Specificity test carried out by interchanging the primers.	60 min	(104)
Escherichia coli O157:H7, *Salmonella typhimurium* and *Vibrio parahaemolyticus*	Centrifugal based platform eliciting a colorimetric change mediated by EBT upon generation of LAMP amplicons.	Spiked DNA samples	380 copies of bacterial DNA.	Carried out via cross-reactivity testing using *E. coli* primers for other pathogenic bacteria.	60 min	(105)
Escherichia coli O157:H7, *Salmonella typhimurium, Vibrio parahaemolyticus* and *Listeria monocytogenes*	Eriochrome Black T (EBT)-mediated colorimetric detection from purple to sky blue in presence of Mg^{2+} metal indicator in a centrifugal system.	Milk samples spiked with bacterial cells.	10 bacterial cells for *E. coli* O157:H7.	None	65 min	(106)
Salmonella	Direct visual observation of the color change of the SYBR Green I dye.	Spiked tomatoes	5×10^{-3} ng/µL DNA concentration	Non-Salmonella strains which include *E. coli, Shigella sonnei, Listeria monocytogenes, Vibrio cholerae, Yersiniae spp. and Acinetobacter baumannii.*	70 min	(107)
Immunoassay						
E. coli	Nanoplasmonics enhanced lens-free interferometric microscopy (LIM) LIM	Blood plasma	400 cells/ml at sample volume of 10 µl	Tested with *Bacillus cereus*	40 min	(108)
E. coli O157:H7	Color change of Horeradishperoxie(HRP), hydrogen peroxide and	Proof of concept	50 CFU/mL	*Listeria monocytogenes* and	60 min	(89)

	tyramine (TYR) system from blue to red	established with meat samples		*Salmonella typhimurium*		
Acinetobacter baumannii (AB)	Horseradish per- oxidase (HRP) and 3,3′, 5,5′-tetra-methylbenzidine (TMB) substrate reaction	In vitro spiked samples	450 CFU per reaction	Verified with MRSA	40 min	(88)
Acinetobacter baumannii (AB), Escherichia coli (EC), and *Staphylococcus aureus (MRSA)*	Horseradish per- oxidase (HRP) and 3,3′, 5,5′-tetra-methylbenzidine (TMB) substrate reaction	In vitro spiked samples	10^3, 10^4 and 10^5 CFU/μL for AB, EC and MRSA, respectively	None	35 min	(109)
E. coli	Fluorescent and colorimetric dual-channel sensing system	Spiked samples and food samples	100 CFU/ml for florescent detection and 44 CFU/ml for colorimetric channel	None	~2 h	(110)
Listeria monocytogenes	Fluorescent gold nanoclusters	Contaminated milk samples	2000 CFU in each 10 μL sample	With three *monocytogenes* strains and two other Gram-positive strains	~50 min	(111)

2.6 Conclusion and Perspectives

While traditional pathogen detection approaches, such as LAMP, PCR, immunocapture, and ELISA, are often sensitive enough, many of them suffer from lengthy response times, lack adequate adaptability for use in remote and isolated settings, and are too costly to support efforts against managing bacteria infections on a wide scale. The direct impact of long waiting times and assay complexity is prominent in remote, isolated, and low-resource communities around the globe. Moreover, the requirement of trained personnel further worsens the applicability of these tests for screening the masses. Colorimetric approaches can rightly address this pressing need. Colorimetric platforms for bacteria detection have shown to be an optimal, affordable, accessible, user-friendly, and time-effective alternative to traditional approaches. The average analysis time for colorimetric detection is ~90 min which is rapid compared to traditional approaches. They also offer room for the seamless integration of sample-to-result automation, which can avoid any user induced errors. All these features allow for decentralizing testing efforts and paving the way for the development of home-based and bedside tests which can be crucial to curb any infectious disease outbreak.

Despite the remarkable progress in colorimetric testing of bacteria, this area of research is not without some limitations. Specifically, for the widespread use of colorimetric microfluidic devices, detection sensitivity has been a major hurdle, which in turn may influence the time to results and the ability to accurately detect samples. Numerous factors influence this sensitivity, but two factors are the most prominent. The first factor is that the human eye is insensitive to low level color contrasts; thus, discriminating outputs between distinct samples is difficult with the naked eye since a majority of conventional colorimetric approaches primarily depend on the colored output's optical density variation (112). The second limiting factor is maintaining the integrity of the colorimetric reagent during prolonged storage periods and during transportation, since these reagents are essential to avoid any false positives and/or negatives (113). Different strategies have been employed to address these challenges like single-step amplification techniques and sensing platforms employing nanomaterials with surface reaction-dependent physicochemical characteristics, particularly, plasmonic nanostructures, as reported in Section 2.5. Recent studies show that different reflectance spectra can be elicited by specialized metal nanostructure arrangements of various dimensions with an incident light source (114). More importantly, a change in the surface analyte's refractive index brings about a change in the colorimetric characteristics of these nanostructures which can simply be analyzed by the naked eye or enabled by a portable optical setup with an inbuilt light source (114). Moreover, the optical properties of these plasmonic nanostructures can be manipulated by varying either the size and shape, making them worth exploring for colorimetric detection applications (114). These inherent features of plasmonic nanostructures offer amazing advantages, particularly high sensitivity in response to external stimuli in comparison to conventional colorimetric assays using organic chromophores (114). Moreover, high sensitivity is linked to the response time and the ability to accurately detect

positive samples. While many reports of colorimetric biosensors show results in ~90 min, this metric may be improved by employing plasmonic nanostructures more widely. Of the reported biosensors, those which have employed plasmonic materials have demonstrated more rapid response times of <50 min (108,111). With growing interest in making existing biosensors truly POC with high sensitivity and throughput, the use of these plasmonic structures can play a crucial role in bridging the gap between colorimetric detection and excellent sensitivity.

Preface to Chapter 3

Chapter 3 discusses the optimization processes that preceded the study in Chapter 4. Primarily, there were three components of our study that needed optimization. This included the number of primers used, DNA extraction protocol, and the concentration of color changing dyes that would ensure the most effective results. These procedures informed the study design in chapter 4 and ultimately ensured that the results adhered to high standards of sensitivity, time-to-results, and applicability for POC settings.

3 Optimization of Study

3.1 Introduction

This chapter describes the optimization steps of the study presented in Chapter 4. Specifically, to reach the results presented in Chapter 4, we tested different primer sets for the colorimetric LAMP assay, methods of DNA extraction, and resazurin concentrations that would be suitable for our study, in order to reach the fastest response time, ensure high specificity and sensitivity of detection, while meeting requirements for POC applications.

3.2 Materials & Methods

3.2.1 LAMP Assay

The LAMP primers used in the optimization studies have been designed and published in a previous study by Oh et. al (1) and were purchased from Sigma-Aldrich.

The LAMP assay included the primer set, DNA sample, WarmStart® Colorimetric LAMP 2X Master Mix (NewEngland Biolabs, MA, USA), and DNAse-free H_2O (Thermo Fischer Scientific, MA, USA). The typical reaction volume of 25 µl consisted of 2.5 µl 10X primers, 12.5 µl WarmStart® Colorimetric LAMP 2X Master Mix, 9 µl DNase-free H_2O, and 1 µl DNA sample. The LAMP reaction was incubated at a temperature ranging from 60-65°C and monitored for color changes at different intervals up to 60 min.

For experiments with resazurin, the LAMP reaction consisted of 12.5 µL of WarmStart® LAMP 2X Master Mix (NewEngland Biolabs, MA, USA), 2.5 µL of 10X primer mix, 9 µL of DNAse-free H_2O (Thermo Fischer Scientific, MA, USA) with a variable concentration of resazurin (0.5 mg/mL, 0.25 mg/mL, and 0.125 mg/mL), and 1 µL of the DNA sample.

3.2.2 Bacterial DNA

We cultured *E. coli* samples overnight at 37℃ in Luria Broth (LB) media. Bacteria concentrations were determined using a Spectronic 21D spectrophotometer. Different concentrations were prepared including 10^7 CFU/mL, 10^5 CFU/mL, 10^4 CFU/mL, 10^3 CFU/mL, 10^2 CFU/mL, and 10 CFU/mL to match physiological concentrations by suspending the *E. coli* cultures in LB media.

DNA was extracted by 4 different methods to determine which condition led to optimal results. Specifically, we extracted DNA using 1) a chemical lysis buffer (Bio Basic Inc., ON, CA) followed by centrifugation of the sample at 1000 RPM, 2) heating the bacteria culture at 95 °C for 10 minutes in an Eppendorf tube in water, 3) heating the bacteria culture followed by centrifugation of the sample, and 4) the lysis buffer alone.

3.2.3 Plasmonic Platform

To create the colorimetric platform, we developed a colloidal self-assembled monolayer (SAM) of polystyrene nanostructures at an air-water interface. The resulting lattice was transferred to a silicon substrate. A 120 nm zinc-oxide film was deposited as a back-reflector and a thin aluminum layer was deposited as the plasmonic surface. This provided a color-tunable area with a white background enabled by surface plasmon resonance.

3.2.4 Imaging & Analysis

All results are based on sampled color matrices from the raw microscopy images from a Nikon Ti Eclipse bright-field microscope. Statistical analysis was conducted using the OriginPro (OriginLab, 2021) software package.

3.3 Optimization Results

3.3.1 LAMP Primer Sets

Initially, we experimented with a set of 4 LAMP primers for *E. coli* as reported in Table 1 based on a study by Oh et. al (1) targeting the *E. coli ycjN* gene.

Table 1: Primer sets and initial concentration of each primer for *E. coli*.

***E. Coli* LAMP Primer Set Targeting *ycjN* Gene**		
Primer	**5' to 3' Sequence**	**Initial Concentration**
F3	ACCTATATCCTTCCGGCTGT	1.1 µM
B3	CACCTGGCGACATCATCAC	1.1 µM
FIP	TCAACATGCCGTAGACCGCAGAACCCGAAAA ACGTCGGTTTC	8.9 µM
BIP	CGGGCAAAAGACCGAAGAGACGCCAGTCGGC AATGTTGTCTG	8.9 µM

Using these primers, we received off-chip color change results of phenol red in 2 hours in a water bath, and in 50 min on the colorimetric platform for a DNA concentration of 70 ng/µL of *E. coli* (Figure 1). Moreover, when tested on the platform, the color change only transitioned to a light pink color rather than orange or yellow, due to a prolonged incubation period needed for visible color change. Upon further investigation, we learned that 6 primers are preferrable compared to 4 primers due to enhanced amplification and in turn, faster time to results (2). Consequently, in future studies we opted to use 6 primers, which led to extremely rapid results, as reported in Chapter 4.

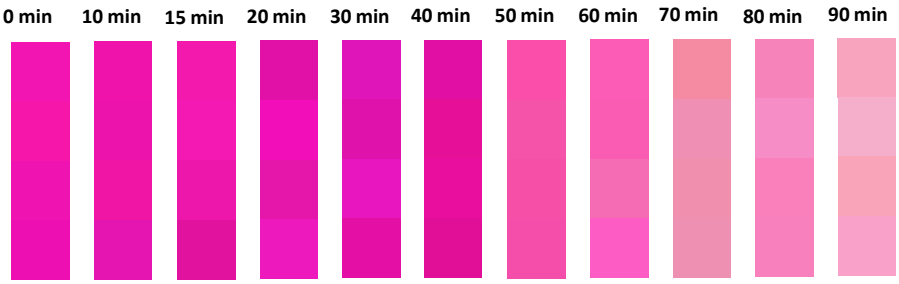

Figure 1: Sampled color matrix of platform results of 70 ng/µL *E. coli* DNA using primer set of 4 primers. Color change is visible from fuchsia to light pink transition at 50 min.

3.3.2 DNA Extraction Protocol

For POC settings, it is imperative that the DNA extraction protocol is simple and accessible, due to the limitation of resources that are available. At the POC, prior studies have applied various DNA extraction protocols such as chemical lysis and heating methods to effectively detect targets (3). Knowing this, we experimented with four different extraction protocols including 1) chemical lysis + centrifugation, 2) heating, 3) heating + centrifugation, and 4) chemical lysis to determine the most preferable mechanism for DNA isolation from *E. coli* cultures. Following these extraction methods, we ran a colorimetric LAMP assay in a water bath in a temperature ranging between 60-65°C, using extracted DNA samples. We found that after a 1-hour incubation period in the water bath, the samples that had been treated with the chemical lysis + centrifugation (Figure 2b) and heating (Figure 2c) methods, exhibited the most prominent color changes compared to negative control (with no DNA) (Figure 2a), heating + centrifugation (Figure 2d), and chemical lysis samples (Figure 2e). Thus, all subsequent DNA extraction protocols involved the heating method, as this is the most favourable option for resource-limited settings, due to affordability and accessibility.

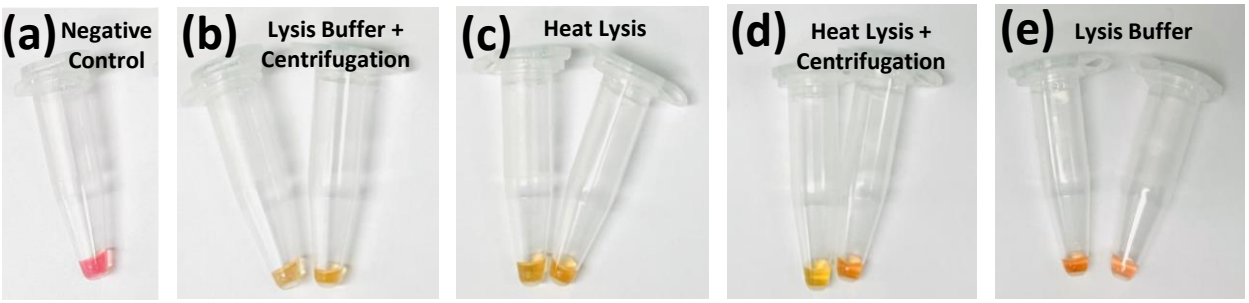

Figure 2: Results of LAMP assay with various DNA extraction protocols. (a) Negative control with no DNA sample. (b) DNA sample with chemical lysis buffer and centrifugation extraction. (c) DNA sample with heat lysis method. (d) DNA sample with heating and centrifugation. (e) DNA sample with chemical lysis buffer extraction alone. The largest color change was exhibited by lysis buffer + centrifugation and heating.

3.3.3 Resazurin Concentration

In our investigation in Chapter 4, in addition to phenol red, we experimented with resazurin as a pH sensitive dye. At a pH of 6.5, resazurin presents itself as dark blue and at a pH of 3.8, resazurin is orange (4). We tested various concentrations of resazurin in our experiments, including 0.125 mg/mL, 0.25 mg/mL, and 0.5 mg/mL to determine the optimal concentration for high color contrast and fast time-to-results. In our tests, we incubated the LAMP cocktail with resazurin dye in an Eppendorf tube in a water bath for various periods of time up to 60 min and visibly monitored color changes (Figure 3a-c). For 0.5 mg/mL, we observed a visible color change from blue to purple at 40 min (Figure 3a). At a concentration of 0.25 mg/mL we observed a color change at 35 min, from blue to lavender (Figure 3b). For 0.125 mg/mL the color change was again observed at 35 min, however the contrast was less noticeable from light blue to light purple (Figure 3c). While all resazurin optimizations studies showed a color change between 35-40 min, 0.25 mg/mL was the most favourable concentration as it exhibited a strong combination of a reasonable response

time and noticeable color contrast from blue to lavender. Thus, for our comparison experiments between resazurin and phenol red dyes in Chapter 4, we opted to use a resazurin concentration of 0.25 mg/mL

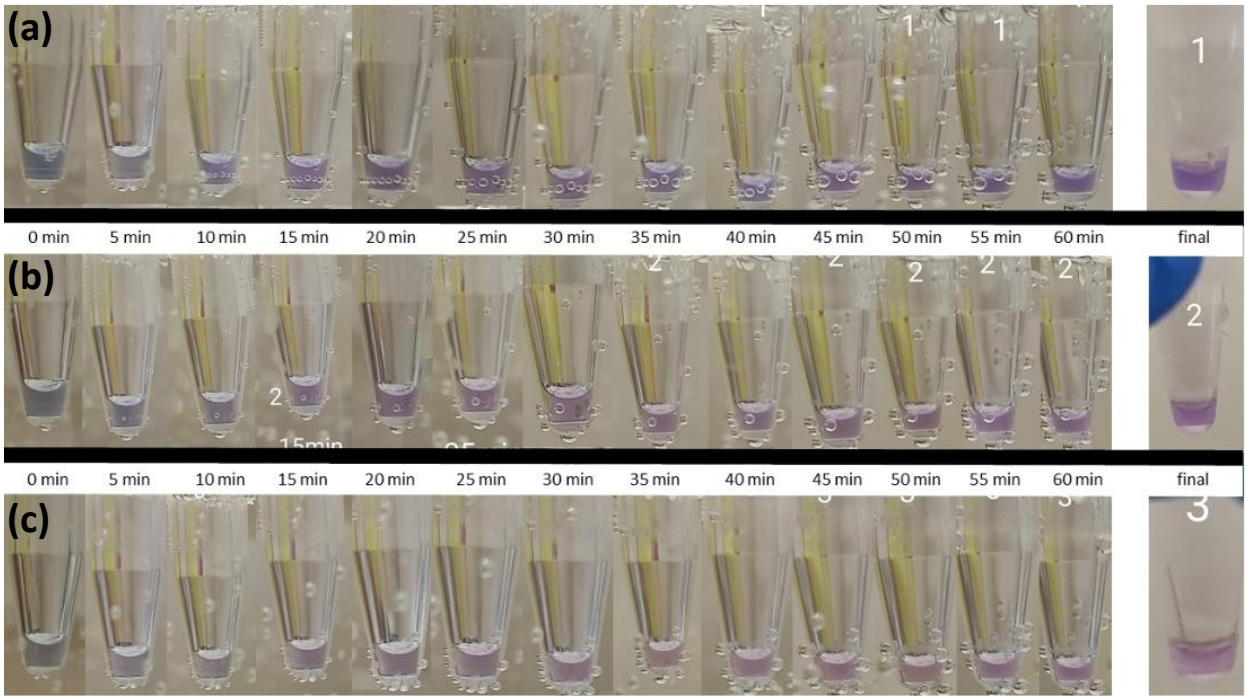

Figure 3: Comparison of concentrations of resazurin. (a) Color response of resazurin-based LAMP cocktail with a resazurin concentration of 0.5 mg/mL. (b) Resazurin concentration of 0.25 mg/mL and corresponding colorimetric response. (c) Colorimetric change of resazurin concentration at 0.125 mg/mL.

3.4 Conclusion

This chapter presented the various experiments that led to the optimization of the study presented in Chapter 4. Overall, we opted to use a set of 6 primers instead of 4, extracted bacterial DNA for *E. coli* using the heat lysis method, and employed a resazurin concentration of 0.25 mg/mL for comparison experiments between phenol red and resazurin. This enabled us to design experiments with optimal sensitivity and rapidity, while enabling applications in POC settings.

3.5 References

1. Oh SJ, Park BH, Choi G, Seo JH, Jung JH, Choi JS, et al. Fully automated and colorimetric foodborne pathogen detection on an integrated centrifugal microfluidic device. Lab Chip [Internet]. 2016 May 10 [cited 2022 Mar 20];16(10):1917–26. Available from: https://pubs.rsc.org/en/content/articlehtml/2016/lc/c6lc00326e

2. Nagamine K, Hase T, Notomi T. Accelerated reaction by loop-mediated isothermal amplification using loop primers. Mol Cell Probes [Internet]. 2002 [cited 2022 Jun 17];16(3):223–9. Available from: https://pubmed.ncbi.nlm.nih.gov/12144774/

3. Dashti AA, Dashti H. Heat Treatment of Bacteria: A Simple Method of DNA Extraction for Molecular Techniques. Artic J Kuwait Med Assoc [Internet]. 2009 [cited 2022 Jun 17]; Available from: https://www.researchgate.net/publication/266888615

4. Moyer R 54, Campbell JJR. M]~CHANISM OF RESAZURIN REDUCTION IN MILK OF LOW BACTERIAL CONTENT. J Dairy Sci. 46:897–906.

Preface to Chapter 4

Chapter 4 presents a prepared manuscript on a novel plasmonic-enhanced biosensor for the detection of bacterial DNA. This study is greatly informed by the literature review and optimization chapters of this thesis (Chapter 2 and Chapter 3). Chapter 2 described the standing need for a biosensor with a faster response time which can detect samples with high sensitivity and accuracy.

To this end, nano plasmonic materials have shown the potential to facilitate high optical sensitivity when combined with colorimetric nucleic acid amplification techniques such as LAMP. This principle is at the heart of our work as we have applied a novel plasmonic-enhanced colorimetric biosensor for the rapid detection of pathogenic bacteria.

Initially, we investigated phenol red and resazurin as color changing dyes for the LAMP assay and studied the electrochemical properties of our biosensor in boosting the LAMP reaction. We applied our biosensor in the detection of three pathogenic bacteria: *E. coli*, Methicillin-resistant *S. aureus*, and *P. aeruginosa*, achieving sample detection as early as 7 min. Our biosensor further achieved a sufficiently low LOD of 0.2 ng/µL. Moreover, each sample demonstrated 100% specificity for target DNA, showing no false-positive or false-negative results.

Overall, our biosensor exemplifies a promising avenue for future POC detection of bacteria, specifically highlighting the value of plasmonic materials in enabling highly sensitive sample detection and fast response times.

4 Ultra-Rapid Detection of Bacterial DNA Using Plasmonic-enhanced Colorimetric Biosensor

Haleema Khan, Tamer AbdelFatah, Mahsa Jalali, Olivia Jeanne, Carolina del Real Mata, Roozbeh Siavash Moakhar, Seyed Vahid Hamidi, Sara Mahshid[*]

Department of Bioengineering, McGill University,
Montréal, QC, H3A 0C3, Canada
E-mail: sara.mahshid@mcgill.ca

4.1 Abstract

Infectious diseases driven by bacteria are a major global health concern and one of the leading causes of death worldwide. The current gold standard bacteria diagnostics techniques, including polymerase chain reaction (PCR) and culturing methods, are complex, expensive, and mainly suited to centralized laboratories. Detection of bacteria using these methods takes between 24-72 hours for definitive results, causing delays in treatment plans, and ultimately worsening a patient's health conditions. The challenge is to reduce the cost and time of the conventional methods, while maintaining their sensitivity and accuracy in bacteria detection. To this end, we have recently proposed QolorEX, a novel molecular testing biosensor integrated with a plasmonic-assisted colorimetric platform, for the direct detection of nucleic acids. This biosensor employs an ultra-rapid colorimetric loop-mediated isothermal amplification (LAMP) assay facilitated by phenol red, to detect nucleic acids. The reaction changes colour in the presence of phenol red due to DNA amplification by the primers, releasing H^+ ions in the process. Enhanced color sensitivity is further boosted by the plasmonic nanostructures under the illumination of bright light, which can be observed using a bright-field microscope or smart imaging box, avoiding the need for complex laboratory equipment or highly trained personnel. Here we adopt these unique properties in the detection of bacterial DNA. We applied this biosensor to detect DNA from *Escherichia coli*,

Pseudomonas aeruginosa, and Methicillin-resistant *Staphylococcus aureus* samples, achieving results in as early as 7 min and within 15 min for all samples, conferring a faster response time compared to the off-chip assay due to plasmonic-assistance. We also tested the *E. coli* DNA in the physiological range in urine samples mimicking urinary tract infections. The biosensor was able to detect all samples in a linear range between 0.2 ng/µL - 50 ng/ µL. The calculated limit of detection was as low as 1.4 ng/µL, which is a highly sensitive response, and matches our observations. Moreover, the primers showed 100% specificity for target DNA. Overall, this study further validates our biosensor, as a robust avenue for nucleic acid detection in a time-sensitive manner, shedding light on the value of plasmonic-assisted color sensing for diagnostics.

Keywords: bacteria diagnosis, plasmonic nanostructures, point-of-care, LAMP, microfluidics

4.2 Introduction

Infections driven by bacteria are a major global health burden and one of the leading causes of death worldwide. Approximately 6.7 million lives are taken globally each year by bacterial infections (1), with the highest impact on low-resource settings (2). Bacteria pathogens including *Escherichia coli* (*E. coli*), Methicillin-resistant *Staphylococcus aureus* (*S. aureus*), and *Pseudomonas aeruginosa* (*P. aeruginosa*), are among the most harmful types of infectious diseases widely (3,4). Moreover, the rise in antibiotic resistance in recent years has exacerbated this issue due to increased rates of morbidity and mortality, greater pressure on public health resources, enhanced risk with surgical procedures due to nosocomial infections, and economic strains (5,6). Several factors can be attributed to the problem of bacteria infections on healthcare systems including significant delays in diagnosis and treatments (7), high cost of diagnostic

instruments (8), and the necessity of well-trained personnel for performing complex clinical tests (9). Furthermore, current gold-standard diagnostic techniques – PCR and culturing methods – have long turnaround times of up to 72 hours for diagnostic results and are rather complex procedures for untrained scientists (10,11). This sheds light on the importance of feasible, timely diagnosis and therapeutic measures to control the spread of infectious diseases driven by bacteria. Point-of-care (POC) diagnostics can address this by rapidly providing test results that can enable healthcare practitioners to prescribe timely therapeutic protocols, for enhanced medical care of patients. In our work, POC diagnostics encompasses nucleic acid-based testing for the accurate detection of bacterial infections, which may be implemented in clinics and the home for effective disease management in the healthcare system.

Isothermal molecular testing has gained significant traction in the POC diagnostic space due to accessible setups and ease of operation. In contrast to standard PCR and culturing methods, loop-mediated isothermal amplification (LAMP) provides a unique method of nucleic acid detection, which obviates the need for a thermal cycler, complex apparatuses, and is rather simple to perform, while maintaining similar sensitivity and specificity results (12,13). LAMP involves using a set of 4-6 primers to amplify target DNA sequences in a rapid time frame of 15-60 min at a temperature ranging from 55-65°C (14,15). This makes LAMP a more suitable, less complicated alternative to PCR while maintaining similar accuracy and sensitivity (16). Another crucial aspect of LAMP is that it can distinguish up to eight specific locations on the target DNA strand due to the use of several primers, compared to only two primers in PCR, leading to highly specific detection of analytes (17). LAMP assays can be complemented by colorimetric readout methods in order to enhance detection for pathogens of interest (18–21), and will be the main approach for nucleic acid amplification in the present study.

Colorimetric readout techniques can seamlessly be implemented in LAMP as they involve affordable reagents, simple readout mechanisms, fast response times, and the ability to detect both negative and positive samples (22,23). Colorimetric assays typically involve the use of color-changing or fluorescent dyes, such as phenol red, calcein, malachite green, and hydroxynaphthol blue, that vary in intensity based on changes in the molecular environment (24–27). The optical sensitivity of colorimetric assays can be further augmented through the resolution of the color pigment that is captured by plasmonic excitation (28).

Plasmonic surfaces such as gold (29), silver (30), and aluminum (31), enable high color tunability when printed on geometric nanostructures such as nanorods, nanocubes, and nanodisks that are smaller than the diffraction limit of light posited by Abbe's Diffraction Limit Theory (32). The combination of nanoparticles and plasmonic surfaces leads to resonance of free electrons at unique wavelengths of light, in a phenomenon called surface plasmon resonance (SPR), generating distinct colors across the visible spectrum, thereby leading to a highly sensitive optical readout (33). This enables rapid sensing of molecular reactions.

Surface plasmon resonance integrated with colorimetric LAMP, facilitates the rapid detection of nucleic acids from pathogens with enhanced optical sensitivity. To this end we have recently proposed QolorEX, a novel colorimetric plasmonic-assisted nucleic acid testing biosensor for the rapid detection of nucleic acids. In our study, nucleic acid amplification from a LAMP reaction can be detected due to the release of H^+ ions, when DNA polymerases incorporate dNTPs to the nascent DNA strand (25,26,34). In the presence of phenol red, a pH indicator which changes color from fuchsia to yellow at a pH of 6.8, the amplification of nucleic acids can be directly monitored (35,36). This phenomenon, coupled with the high color tunability of plasmonic nanostructures enables ultrasensitive, rapid detection (37). Colorimetric LAMP assays combined

with plasmonic nanostructures have previously been applied in the detection of tuberculosis (38), influenza (39), and Methicillin-resistant *S. aureus* (40), positing a robust technique for nucleic acid detection in a time-sensitive manner.

In this investigation we applied a modified version of QolorEX to diagnose DNA from three pathogenic bacteria: *Escherichia coli (E. coli)*, Methicillin-resistant *Staphylococcus aureus (S. aureus)*, and *Pseudomonas aeruginosa (P. aeruginosa)* (Figure 1). We demonstrated that phenol red is an excellent colorimetric indicator for its fast response time and high color contrast, compared to other dyes. Moreover, we demonstrated that the amplification reaction is boosted through plasmonic enhancement, based on the transfer of electrons into the media, leading to a reduction in the colorimetric response time by at least 15 min compared to the standard colorimetric assay. We were able to detect bacterial DNA from all three pathogens in the physiological range from 0.2 ng/µL - 50 ng/µL within 15 min, and as early as 7 min. The primers used showed no cross-reaction with other bacterial DNA, demonstrating 100% specificity. We also tested the *E. coli* DNA in the physiological range in urine samples, mimicking urinary tract infections. Overall, our approach is a rapid DNA diagnostic technique compared to conventional PCR and culturing methods. This study also sheds light on the value of surface plasmon resonance as a method of enhancing color sensitivity for conventional colorimetric readouts in POC applications. We achieved a faster response time within 7 min due to plasmonic enhancement, compared to a 30-min assay response as seen by the naked eye. Moreover, this study further validates the efficacy of our biosensor for ultra-rapid nucleic acid detection in a range of clinical applications.

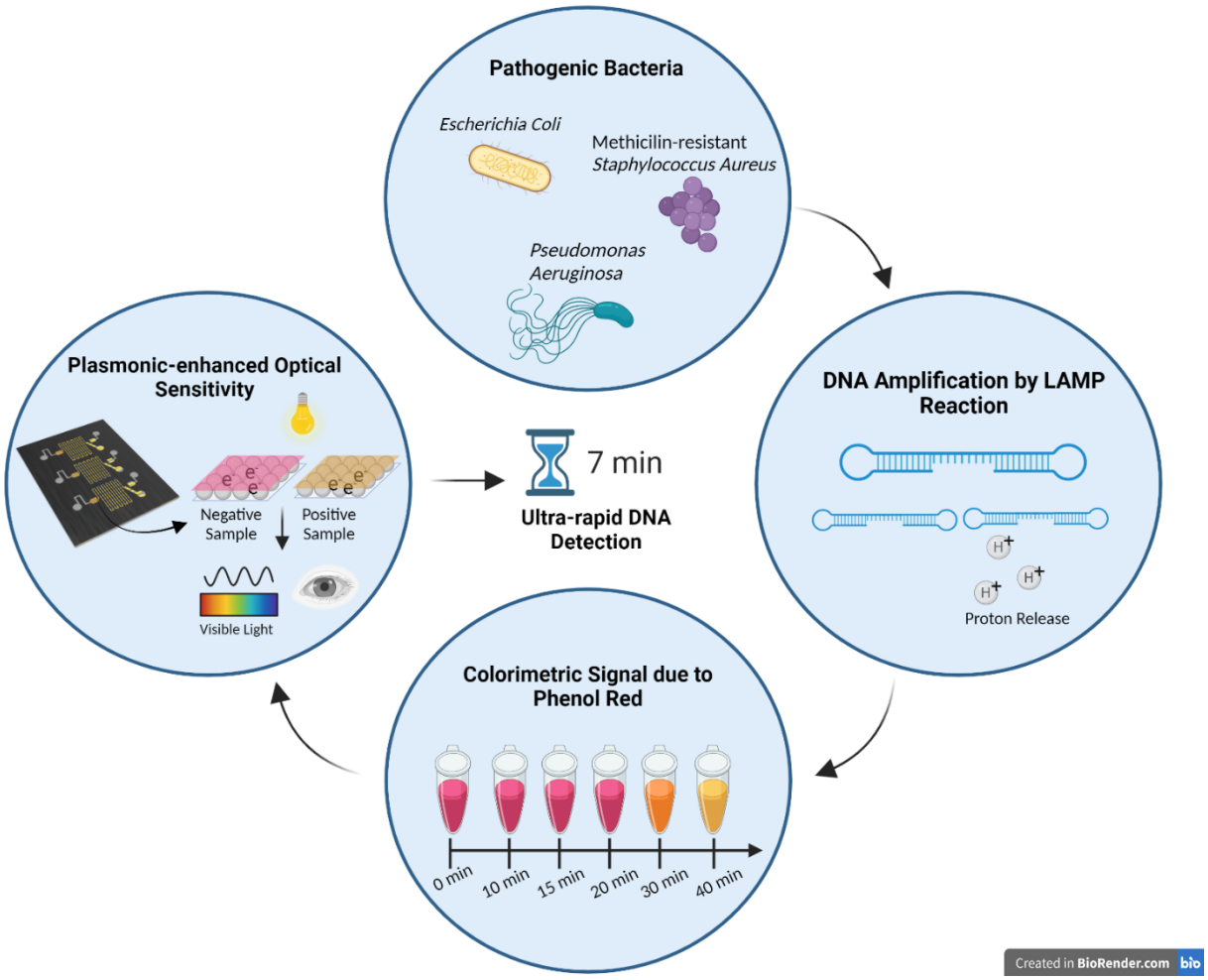

Figure 1: Schematic of colorimetric LAMP assay combined with plasmonic nanoparticles integrated in microfluidic biosensor for rapid and sensitive detection of bacterial DNA for *E. coli*, Methicillin-resistant *S. aureus*, and *P. aeruginosa*. Created with BioRender.com.

4.3 Materials & Methods

4.3.1 LAMP Assay

Three different sets of LAMP primers were used in this study for the corresponding pathogenic DNA samples as shown in Table S1. The primers have been designed and published in previous studies by Hill *et al.* (41), Chen *et al.* (42), and Goto *et al.* (43) for the *E. Coli malB*

gene, Methicillin-resistant *S. Aureus mecA* gene, and *P. Aeruginosa oprL* gene, respectively. All three primer sets were purchased from Sigma-Aldrich.

The standard LAMP reaction consisted of four components: the DNA sample, 10X primer mix for the individual DNA samples, WarmStart® Colorimetric LAMP 2X Master Mix (NewEngland Biolabs, MA, USA), and DNAse-free H_2O (Thermo Fischer Scientific, MA, USA). The standard reaction volume of 25 µl consisted of 2.5 µl 10X primer mix, 12.5 µl WarmStart® Colorimetric LAMP 2X Master Mix, 9 µl DNase-free H_2O, and 1 µl DNA sample. The LAMP reaction was incubated at a temperature ranging from 60-65°C and monitored for color changes at different intervals up to 60 min.

In the experiments with resazurin the LAMP reaction consisted of 12.5 µL of WarmStart® LAMP 2X Master Mix (NewEngland Biolabs, MA, USA), 2.5 µL of 10X primer mix, 9 µL of DNAse-free H_2O (Thermo Fischer Scientific, MA, USA) with 0.25 mg/mL of resazurin, and 1 µL of the DNA sample.

4.3.2 Bacterial DNA

E. coli samples were cultured overnight at 37℃ in Luria Broth (LB) media. Next, the bacteria concentration was determined using a Spectronic 21D spectrophotometer. Aliquots of different concentrations of 10^7 CFU/mL, 10^5 CFU/mL, 10^4 CFU/mL, 10^3 CFU/mL, 10^2 CFU/mL, and 10 CFU/mL were prepared to match physiological concentrations by suspending the *E. coli* cultures in LB media. *E. coli* DNA was extracted using the boiling method at 95°C for 10 min. Methicillin-resistant *S. aureus* and *P. aeruginosa* DNA was obtained from the McGill University Health Centre using the chemical lysis method to extract DNA. All DNA sample concentrations were measured using a Nanodrop™ 2000 Spectrophotometer and suspended in Universal Buffer

(Bio Basic Inc., ON, CA) to achieve desired concentrations. Spiked urine experiments were carried out using pooled human urine (Innovative Research, MI, USA).

4.3.3 Plasmonic Microfluidic Biosensor

The plasmonic microfluidic biosensor has been previously reported in our prior study (in preparation) and comprises of 4 main elements: 1) sample loading port with an integrated sample filter, 2) the assay loading port and mixing channels for on-chip sample and reagent mixing, 3) plasmonic color-readout window with a color-sensitive platform, and 4) an integrated heater element for LAMP reactions. The fab-flow of the biosensor is reported in detail in Figure S1. For bacteria DNA in buffer, the LAMP mixture was loaded through the assay loading port, as all reagents were mixed off-chip prior to injecting in the biosensor. For *E. coli* in urine, the DNA sample was loaded through the sample loading port, while the remaining LAMP cocktail was loaded in the assay loading port. All ports were covered with a thin film of tape to prevent leakage and evaporation prior to heating the biosensor. Next, a DC power supply was connected to the biosensor and fine-tuned for a temperature reading of 60-65°C (Figure S2). We used a FLIR One Pro infrared camera connected to a smartphone to monitor the temperature throughout the experiment. Finally, the colorimetric signal was monitored from the plasmonic color-sensitive window up to 60 min using a Nikon Ti Eclipse microscope.

4.3.4 Image Processing and Data Extraction

Platform images were acquired at regular intervals from 0-60 min. We used a deep learning algorithm to pre-process the images. Initially, 20% of the images were cropped to remove the coffee ring effect. Next, hue values ranging from 85 to 140, falling within the blue range, were removed, and replaced by the mean of the rest of the image. The bottom ¼ of the parts with lowest

saturation were removed and replaced with the mean value of the rest of the image. In the final step, the image was broken down into 20 mini-images and several features were extracted including mean color values in each color channel – R, G, and B.

4.3.5 Electrochemical Studies

We used a conventional three-electrode cell combined with an Autolab PGSTAT204 potentiostat/galvanostat to perform the electrochemical studies. The microfluidic biosensors were used as the working electrode with Ag/AgCl and platinum wire as the reference and counter electrodes, respectively. We employed a chronoamperometry technique under chopped ambient light (light ON/OFF cycles of 5 s) at a bias potential of 1 V vs. Ag/AgCl in an aqueous LAMP assay. In comparison to the reference electrode, cyclic voltammetry tests ranged in potential from -1 to 1V with a scan rate of 50 mV/s. For all tests we used the standard LAMP assay volumes with *E. coli* DNA in buffer or *E. coli* DNA spiked in human pooled urine.

4.3.6 Statistical Analysis

All results are based on the mean colorimetric signal ± the standard deviation for experiments repeated three times. Statistical analysis was conducted using the OriginPro (OriginLab, 2021) software package. The LODs were calculated through the linear regression method using the slope and standard error of the intercept. A one-way analysis of variance (ANOVA) with *post-hoc* Tukey's test for mean comparison was used to evaluate statistical significance, where datasets with $p<0.05$ were considered statistically significant.

4.4 Results

4.4.1 Features of Plasmonic-enhanced Colorimetric Biosensor

An ultra-rapid colorimetric biosensor integrating a colorimetric LAMP assay, on-chip heating, and plasmonic-enhanced color-sensitive platform was developed for rapid detection of pathogenic bacterial DNA. The biosensor is a user-friendly chip which can be connected to a DC power supply and bright field microscope, to modulate on-chip temperatures and monitor color changes (Figure S2). In addition to rapidity, the biosensor harnesses ease-of-operation and portability, enabling its application in point-of-care settings.

The biosensor employs a pH-driven LAMP assay for the rapid detection of nucleic acids by utilizing a set of 6 primers (Table S1). Initially, the inner primer, FIP, hybridizes to the target DNA at F2c and begins the synthesis of the complementary DNA strand (Figure 2a). The outer primer, F3, then hybridizes to F3c, causing the release of the FIP complementary strand which forms a loop structure. The loop structure acts as a template for BIP to synthesize a complementary strand, which is later displaced by B3-initiated synthesis. This leads to a double-looped (dumb-bell) DNA structure, which serves as a template for exponential amplification by loop primers. In the presence of target DNA, the primers begin to anneal and amplify the DNA at a constant temperature of 60-65°C (Figure 2a). As nucleotides are added to the nascent DNA strand by DNA polymerase, H^+ ions are released in the medium (44), which causes a change in the pH due to acidic conditions. We used phenol red as a pH indicator to monitor the progression of the reaction and increase of the concentration of amplicons.

To enhance the sensitivity of the phenol red LAMP assay, we employed a plasmonic color-sensitive platform. The features of the plasmonic nanostructures including the diameter and the refractive index of the surrounding medium, strongly influence the reflected color of the plasmonic platform (45). We investigated the color of the medium over different diameters of plasmonic nanostructures ranging from 100-750 nm, identifying that the nanoparticle lattice comprised of

400 nm nanoparticles, demonstrated a large color gamut between fuchsia-yellow colors based on the colorimetric signal defined in section 4.4.2 (Figure 2b). This was complemented by an optical UV-visible study to illustrate the absorption wavelength variation when changing the acidity between 8.2 to 6.2 across a 60 min time span (Figure 2b). The platform was fabricated on a silicon (Si) substrate through a fabless self-assembled monolayer using polystyrene nanobeads (Figure 2c). The tightly packed hexagonal lattice of nanobeads was used to fabricate the plasmonic surface by deposition of a zinc-oxide (ZnO) back-reflector and a thin aluminum (Al) plasmonic film in a 120:10 nm ratio. ZnO was deposited in a 0.5 A/s rate onto the polystyrene nanobeads and annealed at 60°C, creating a biocompatible film. To actualize the plasmonic surface, Al was deposited at a 1 A/s rate to produce a uniform reflective layer. Upon illumination of white light, electrons are excited at the interface between the plasmonic substrate and LAMP reaction, causing the reflection of vivid colors. This is the backbone of the optical detection phenomenon of our device. Figure 2c portrays the scanning electron microscope image of the 400 nm self-assembled monolayer nanostructures. In the present study, DNA amplification was evaluated using the 400 nm plasmonic nanostructures integrated in a microfluidic biosensor (Figure 2c).

The biosensor employed here has been previously reported and includes fluidic elements and 4 attached layers (Figure 2c). The device is composed of a silicon wafer, an aluminum heater element to carry out the LAMP reaction, fluidic channels for sample flow, and a PDMS seal securing samples in place. To investigate the sensitivity and specificity of the biosensor in detecting bacterial DNA, a thorough study was performed using bright-field microscopy.

The experimental workflow involved three main steps as illustrated in Figure 2d: 1) the LAMP cocktail was injected in the microfluidic biosensor, 2) the biosensor was connected to a DC

power supply and fine tuned to heat the sample in the desired range based on an infrared camera, and 3) at regular intervals, the biosensor was imaged using a bright-field microscope.

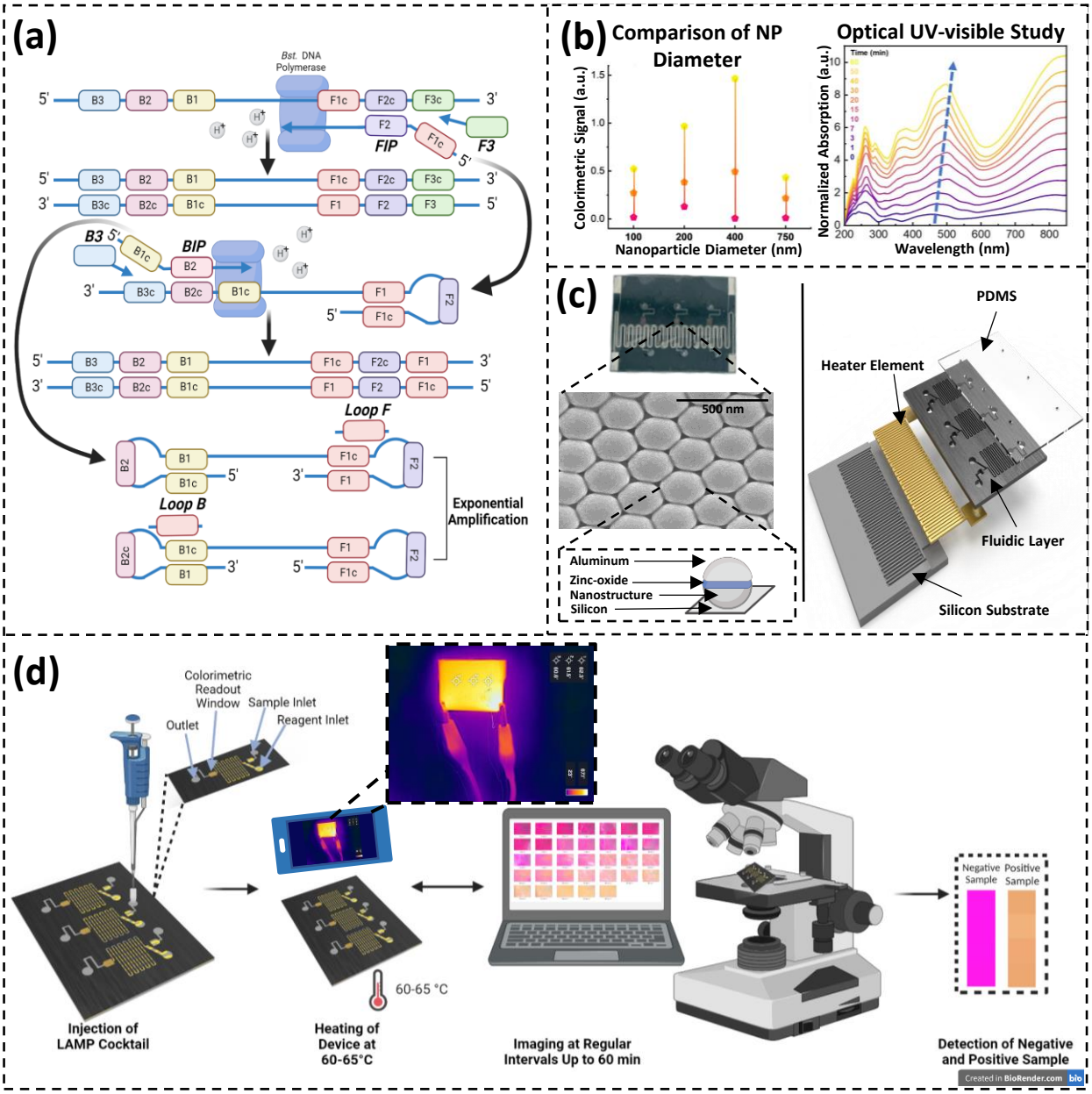

Figure 2: Features of plasmonic-enhanced colorimetric biosensor. (a) Steps of LAMP assay. (b) (Left) Comparison of nanoparticle diameter and colorimetric signal response. (Right) UV-visible study of plasmonic nanostructures with media from pH of 8.2 to 6.2 across 60 min. (c) (Left) SEM image of 400 nm plasmonic nanoparticle lattice, integrated in colorimetric readout window of

biosensor. Each nanoparticle is fabricated on a silicon substrate and coated with a thin layer of aluminum and a zinc-oxide back-reflector. (Right) Image of fluidic biosensor and layers which consist of silicon substrate, embedded heater element, fluidic layer with channels, and PDMS seal. (d) Experimental workflow including injection of LAMP cocktail, heating and temperature monitoring through infrared camera, and bright-field microscopy. Created with BioRender.com.

4.4.2 Comparison of Phenol Red and Resazurin Colorimetric Response

The color-changing dye can have drastic effects on the results of colorimetric assays, as this can impact the time-to-results and optical sensitivity. Initially, we compared the colorimetric response of two pH indicators – phenol red and resazurin – in a LAMP assay with *E. coli* DNA. Phenol red is often used as a colorimetric indicator for nucleic acid amplification due to its sensitivity to H^+ ions. Above a pH of 8.2, phenol red exhibits a fuchsia color and between 8.2 and 6.2, phenol red shows a gradual transition from red to yellow due to the addition of a hydroxyl group (Figure 3a) (36). Thus, in the presence of a positive sample, the increased proton concentration from DNA amplification changes the color of phenol red to yellow (36), enabling the detection of amplicons. In contrast, resazurin exhibits a gradual shift between dark blue and orange from a pH of 6.5 to 3.8, from increasing proton concentrations (Figure 3b) (46). This is due to the loss of an oxygen atom and reduction to the resorufin state (47).

In an experiment of both colorimetric indicators, we first tested the off-chip response times with *E. coli* DNA at a concentration of 70 ng/µL. In brief, the LAMP cocktail was prepared in an Eppendorf tube and incubated at a steady temperature of 60-65°C in a water bath for different time intervals up to 60 min. We noticed color changes at 30 min for phenol red and 35 min for resazurin (Figure 3c-d, Figure S3). Following this, we tested concentrations from 0.2 ng/µL-70 ng/µL on

the colorimetric platform/biosensor using both indicators and captured images at various incubation periods using a bright-field Nikon microscope (Figure 3e-g). Figures 3e and 3g illustrate a matrix of sampled colors from the raw bright-field microscopy images at each time interval up to 60 min. Between 3-5 images were captured at each time interval, rendering a wide color gamut from fuchsia to orange or blue to green in the presence of target DNA. For resazurin, we can observe a color change from blue to green as the initial color of the plasmonic nanostructures appear green under the bright-field microscope.

We compared the response times of both indicators based on visible color changes and corresponding quantitative colorimetric signals. For the phenol red LAMP assay, the images were pre-processed using a deep learning algorithm and mean values in each color channel (R, G, and B) were extracted from the raw images, in order to quantify the colorimetric signal. The colorimetric signal (a.u.) was defined as $\frac{(Average\ green\ value)^2}{(Average\ red\ value)\times(Average\ blue\ value)}$, using the mean values. We defined the colorimetric signal based on increasing mean G values and decreasing mean R and B values for positive tests. In the case of resazurin, we plotted the mean G/B (α) values from the average values of the sampled color matrices (Figure S4c). Phenol red showed visible color changes within 7 min for high concentrations and 15 min for low concentrations, which was supported by a spike in the colorimetric signal (Figure S4a,b). In the resazurin experiments, we observed noticeable color changes from blue to green in 25 min for high concentrations and 55 min for low concentrations which was evident by the spike in α values (Figure S4c).

Although the color change was evident using resazurin as an indicator, the results were slower to appear in comparison to phenol red, especially for low concentrations which is to be expected due to the lower pH requirement of resazurin for visible color changes in the media

(Figure 3f) (47). Moreover, the color change for resazurin is not as striking, requiring a sharper eye for detection. For these reasons we opted to use phenol red as an indicator due to its faster results and more noticeable color change in subsequent experiments.

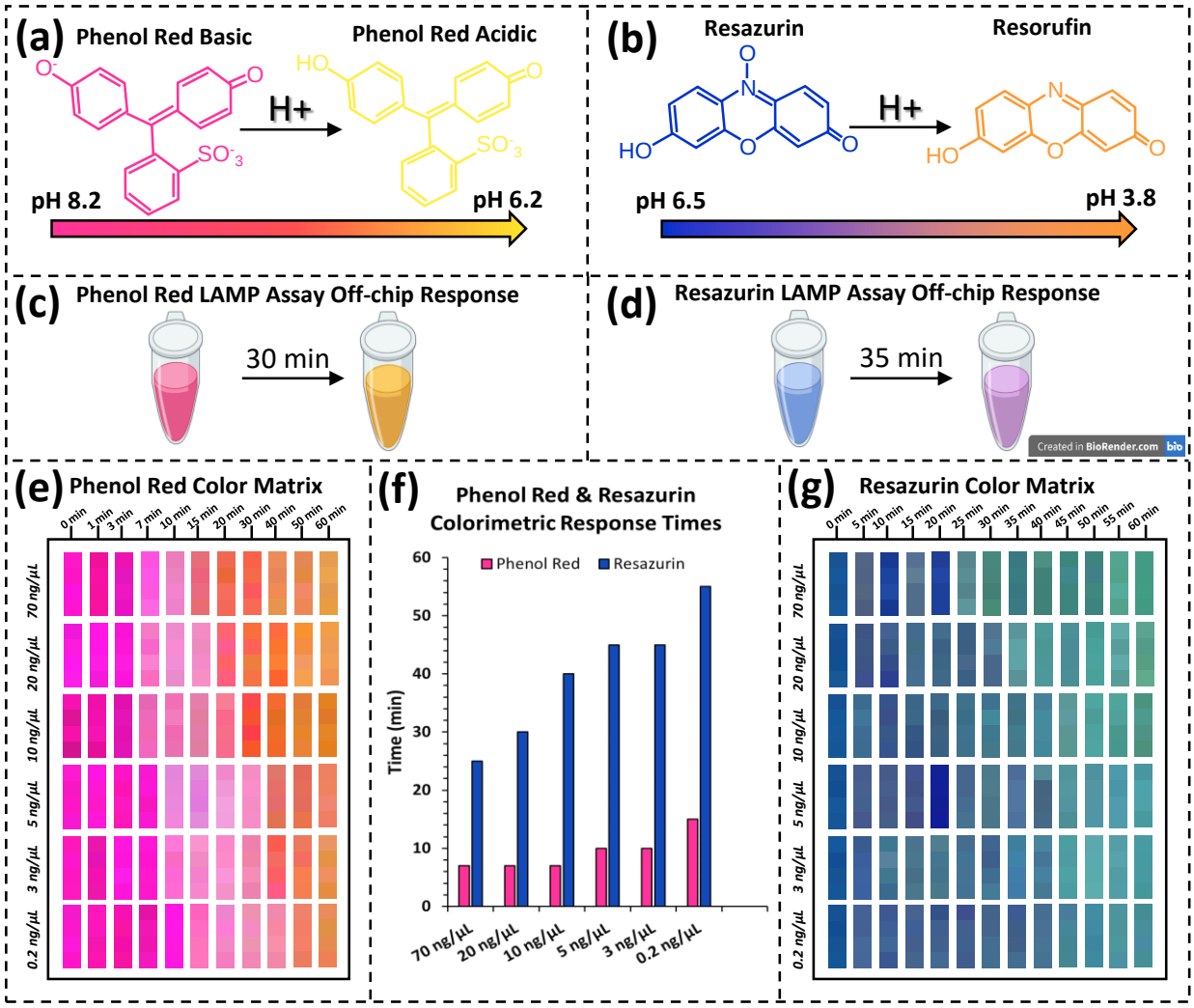

Figure 3: Comparison between colorimetric response of phenol red and resazurin. (a) Conformational change of phenol red based on acidic conditions, leading to shift from fuchsia to yellow from a pH of 8.2 to 6.2. (b) Loss of oxygen atom from increased proton concentrations, leading to change from resazurin to resorufin between a pH of 6.5 and 3.8. (c) Off-chip color change of phenol red observed at 30 min in positive LAMP assay. (d) Off-chip color change of resazurin observed at 35 min in positive LAMP assay. (e) Sampled color matrix of phenol red

LAMP assay tested at various concentrations in colorimetric biosensor. (f) Comparison of response times across tested concentrations for phenol red and resazurin assays. (g) Sampled color matrix of resazurin LAMP assay images on colorimetric platform. Created with BioRender.com.

4.4.3 Electrochemical Studies

Plasmonic resonance relies on electromagnetic field enhancement which is facilitated by incident light (48). This enables the transfer of free electrons into the media which can engage with the amplification reaction, and lead to faster results (49). We investigated the electrochemical properties of the colorimetric biosensor and its potential impact on the amplification reaction through an electrochemical study in the presence and absence of incident light (where light was ON and OFF). Real-time chronoamperometry revealed that electron transfer occurred only in the positive state (where the target nucleic acid was present), under incident light, supporting the idea that electrons play a role in the progression of the amplification reaction (Figure 4a). In a cyclic voltammetry study, we assessed the oxidation current peaks in buffer and urine for both positive and negative samples (Figure 4b). This validated that oxidation current amplification peaks were highest for positive samples under light illumination for both buffer and urine. Electrochemical impedance spectroscopy showed that the positive samples under illumination of incident light, were in the influence of lower surface resistance in comparison to negative samples for both buffer and urine (Figure 4c). Generally, these experiments showed that greater electron transfer occurred in positive samples under bright light illumination, leading to the interaction of electrons with the nucleic acid amplification reaction and enhancing results.

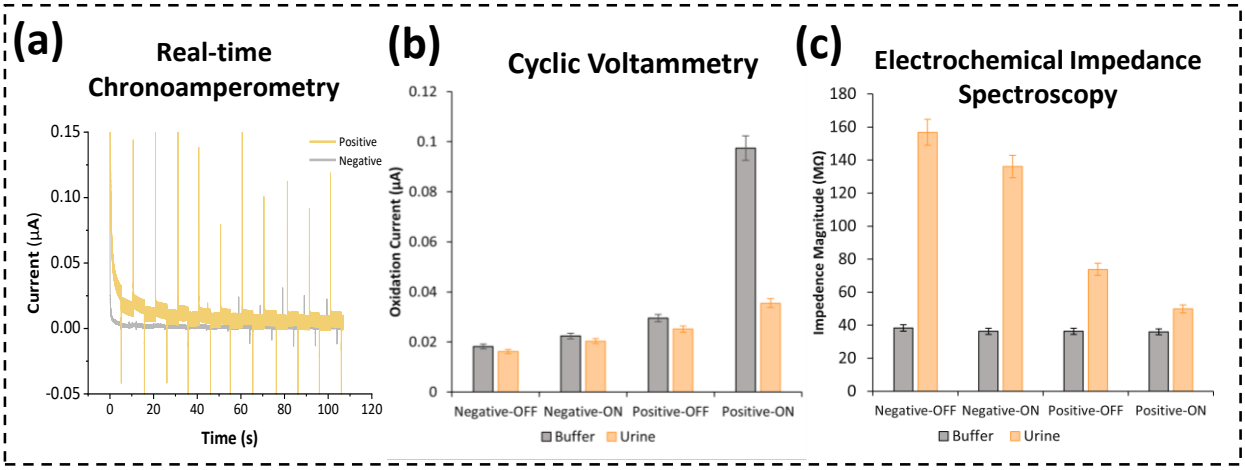

Figure 4: Electrochemical studies of the plasmonic effect from colorimetric platform. (a) Real-time chronoamperometry study of electron transfer in LAMP assay under incident light source. (b) Cyclic voltammetry study of oxidation current peak in buffer and urine in positive and negative reaction conditions. (c) Electrochemical impedance spectroscopy of greater electron transfer under illumination, with lower resistance, in presence of positive samples. Error bars represent 5% relative error.

4.4.4 Specificity

The LAMP primer sets were first validated through off-chip experiments in a water bath where the LAMP cocktail was prepared in an Eppendorf tube and incubated at a steady temperature of 60-65°C for different periods up to 60 min. We tested each pathogenic bacteria sample (*E. coli*, Methicillin-resistant *S. aureus*, and *P. aeruginosa*) at a DNA concentration of 50 ng/μL. Negative controls samples were prepared without DNA, but with the remaining components of the LAMP cocktail. We assessed the off-chip response of DNA amplification by monitoring the color change of each reaction in the presence of phenol red. Figure 5a shows the off-chip response of the LAMP cocktail from 0-60 min for each pathogen compared to negative control samples. Off-chip color changes from fuchsia to yellow were noticeable for each sample at 30 min.

Next, we investigated the specificity of each primer set in the colorimetric biosensor through a cross reactivity test with the target DNA sample, the two non-target DNA samples, and a negative control sample without DNA. The DNA concentrations for individual bacteria samples were 50 ng/µL. For this experiment all primer sets for each pathogen (*E. coli*, Methicillin-resistant *S. aureus*, and *P. aeruginosa*), specifically reacted with target DNA, exhibiting no cross-reactions with non-target DNA or negative control samples. Visibly, target-specific primers led to a rapid color change within 7 min, as identified by a gradual color change from fuchsia to light pink (Figure 5b). In contrast, non-target DNA samples and negative controls remained fuchsia.

Figure 5c depicts the colorimetric signal for the specificity cross reaction for each pathogen. Evidently, the target DNA for each primer set shows an increased colorimetric signal within 60 min. We were able to identify a spike in the colorimetric signal as early as 7 min for concentrations of 50 ng/µL. At 7 min, the response surpassed a colorimetric signal of 0.1 a.u., helping us to identify this as a signal threshold for positive samples. Non-target DNA and negative controls remained below the 0.1 a.u. signal threshold throughout the 60 min test. These quantitative results validated the qualitative responses seen in the microscopy images.

A comparison of the colorimetric signal was evaluated specifically at 15 min, corresponding to the detection time for low concentrations, using a one-way analysis of variance (ANOVA) with a *post-hoc* Tukey's test. Significant differences were observed for the colorimetric signal for the target DNA compared to the non-target DNA and negative control for *E. coli*, Methicillin-resistant *S. aureus*, and *P. aeruginosa*, ($p < 0.001$) (Figure 5d).

In general, the primer sets exhibited 100% specificity for correctly responding to only target DNA samples, showing no cross reactions with non-targets or negative control samples.

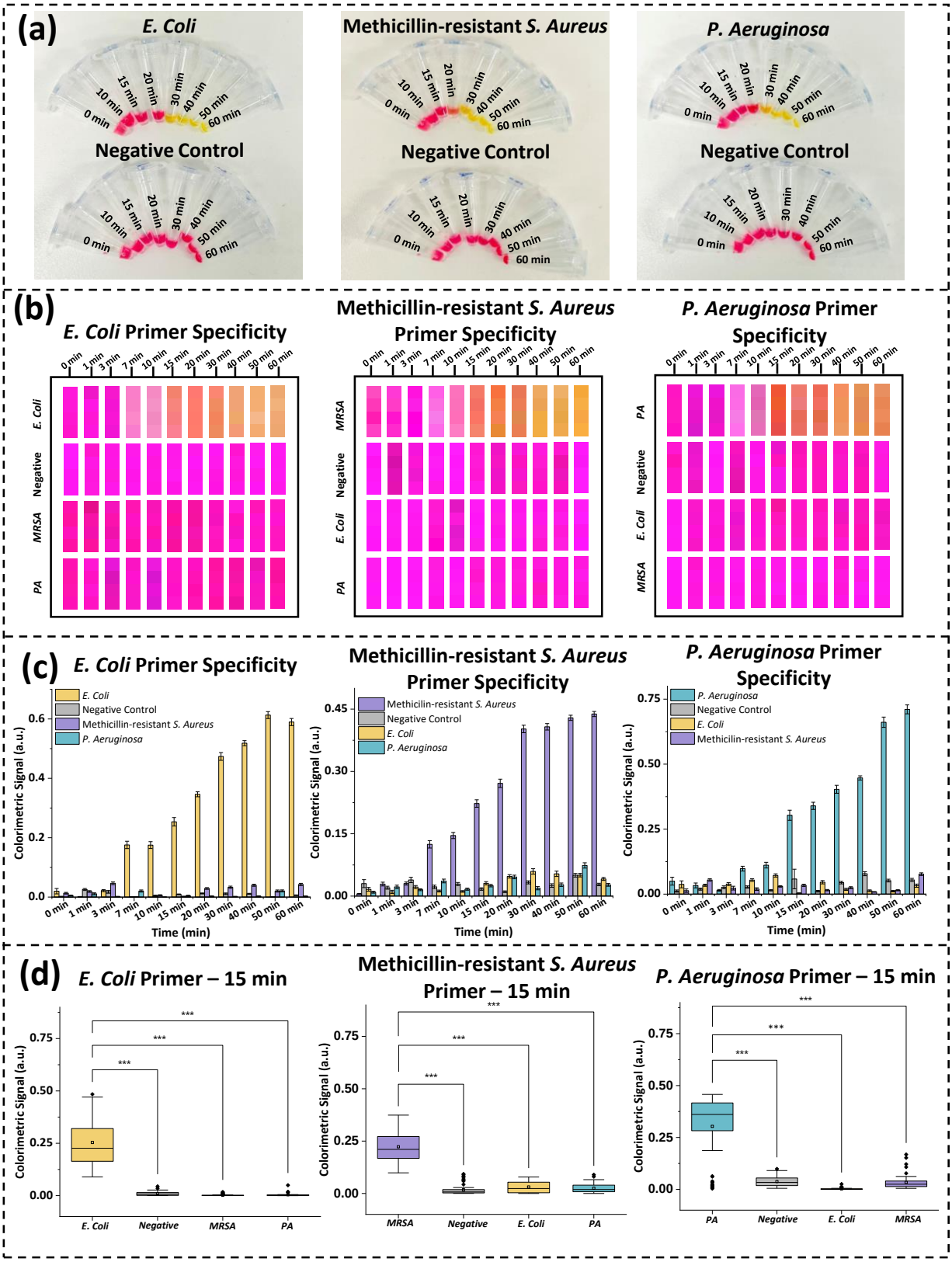

Figure 5: Specificity results of LAMP primers for *E. coli*, Methicillin-resistant *S. aureus*, and *P.*

aeruginosa. (a) Off-chip results of LAMP assay in water bath for each sample up to 60 min. (b) Color matrices of on-chip cross reactivity tests for *E. coli*, Methicillin-resistant *S. aureus* (MRSA), and *P. aeruginosa* (PA) primer sets up to 60 min. (c) Quantitative change in the colorimetric signal for cross reactivity test for each bacterial primer set, showing all target-specific primers led to increase in colorimetric signal past threshold of 0.1 a.u. (d) Comparison of colorimetric signal at 15 min for the cross reactivity test of each bacterial primer set. All target-specific primers showed significant differences with non-target DNA samples and negative controls ($p<0.001$).

4.4.5 Sensitivity of Proposed Biosensor

In our next experiments we evaluated the sensitivity of the biosensor in detecting the physiological range of bacteria samples, which we used in order to graph a calibration curve and identify the limit of detection (LOD). *E. coli* in urine presents itself in the range of 10^2 - 10^5 CFU/mL, in urinary tract infections (50). For our experiments, the extracted DNA concentrations were 70 ng/µL, 50 ng/µL, 20 ng/µL, 10 ng/µL, 3 ng/µL, and 0.2 ng/µL, corresponding to 10^7 CFU/mL, 10^5 CFU/mL, 10^4 CFU/mL, 10^3 CFU/mL, 10^2 CFU/mL, and 10 CFU/mL, respectively. This allowed us to prepare and test *E. coli* DNA samples in the range of 0.2 ng/µL - 70 ng/µL (Figure S5).

For Methicillin-resistant *S. aureus*, the physiological DNA concentration averages between 40-50 ng/µL in nasopharyngeal samples of infection (51), while *P. aeruginosa* presents itself in the range between 10-100 ng/µL in patient sputum samples (52). To test these bacteria, we prepared DNA samples in the range of 0.2 ng/µL - 50 ng/µL (Figure S5).

Figure 6a illustrates a color matrix of sampled colors from the raw microscopy images of on-chip LAMP sensitivity experiments. The highest DNA concentration of 50 ng/µL displayed a

color change at 7 min, as evidenced from a visible transition in colour from fuchsia to light pink. In contrast, DNA concentrations of 0.2 ng/µL showed a color change at 15 min. As expected, this pattern was observed for all three bacteria, due to similar off-chip response times. We plotted the colorimetric signal change at 50 ng/µL for all three bacteria, confirming that a spike in the colorimetric signal change occurred at 7 min as the signal passed 0.1 a.u., validating the observed qualitative responses (Figure 6b).

To determine the limit of detection (LOD), we compared the means of the colorimetric signal at 15 min for each tested concentration. Figure 6c depicts the range of data points for the mean colorimetric signals, indicating a gradual increase in signal for increasing concentrations. We averaged the mean data points per concentration, for each bacterium and plotted a standard curve (Figure 6d). The adjusted R^2 values were 0.99075, 0.96331, and 0.95655, for *E. coli*, Methicillin-resistant *S. aureus*, and *P. aeruginosa*, respectively. The LOD was calculated using values obtained from the standard curve including the standard deviation of the y-intercept, and the slope of the curve as defined by $\frac{3.3 \times Standard\ Deviation}{Slope}$. The LOD was determined to be 1.4 ng/µL for *E. coli*, 2.2 ng/µL for Methicillin-resistant *S. aureus*, and 2.94 ng/µL for *P. aeruginosa*, closely matching the observed 0.2 ng/µL LOD.

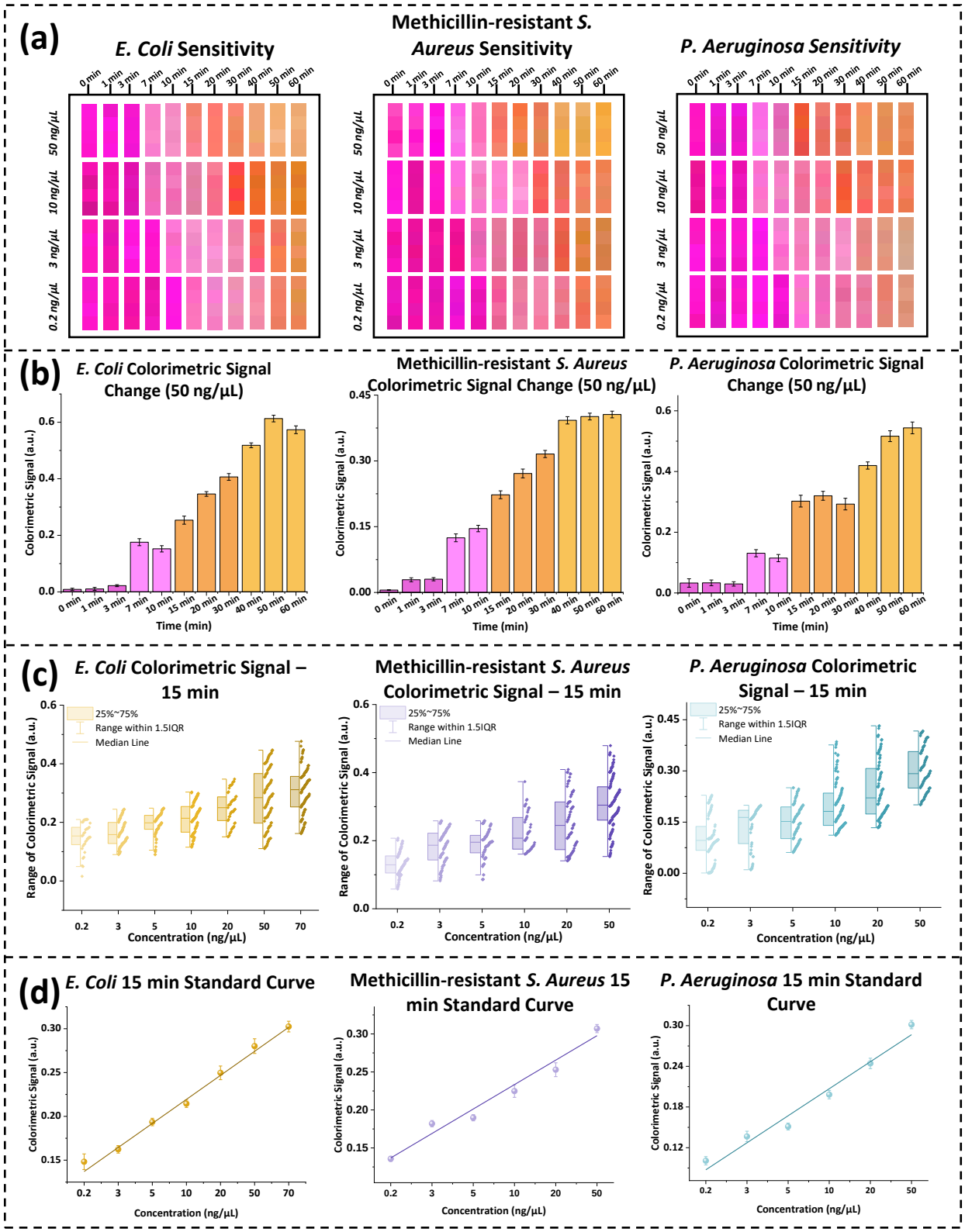

Figure 6: Sensitivity results for *E. coli*, Methicillin-resistant *S. aureus*, and *P. aeruginosa*. (a) Sampled color matrices of on-chip sensitivity test for each bacterial DNA for 0.2 ng/μL, 3 ng/μL,

10 ng/µL, and 50 ng/µL. (b) Quantitative colorimetric signal change for 50 ng/µL. All bacterial DNA showed large signal change at 7 min, passing 0.1 a.u. signal threshold. (c) Range of colorimetric signal for each bacterial DNA concentration at 15 min. Increasing concentrations showed disparity in colorimetric signal. (d) Standard curve for colorimetric signal across 0.2 - 70 ng/µL for *E. coli* and 0.2 - 50 ng/µL for Methicillin-resistant *S. aureus* and *P. aeruginosa*. Adjusted $R^2 = 0.99075$ for *E. coli*, adjusted $R^2 = 0.96331$ for Methicillin-resistant *S. aureus*, and adjusted $R^2 = 0.95655$ for *P. aeruginosa*.

4.4.6 Biosensor Sensitivity in Urine Samples

E. coli typically presents in urine in the range of 3 - 50 ng/µL for urinary tract infections (UTI) (50). To simulate real clinical samples of UTI, we spiked the *E. coli* DNA in 1 µL of pooled human urine. We tested *E. coli* DNA samples in urine across the physiological range on-chip, with noticeable color changes as early as 3 min for 70 ng/µL (Figure 7a). We plotted the colorimetric signal for 70 ng/µL, which confirmed the qualitative response from the on-chip microscopy images (Figure 7b). The standard curve for *E. coli* in urine was plotted as shown in Figure 7c, with an adjusted R^2 value of 0.9868. We used the standard curve to calculate the LOD using the formula $\frac{3.3 \times Standard\ Deviation}{Slope}$ as described in section 4.4.5 which worked out to be 1.73 ng/µL, closely matching *E. coli* in buffer results and the observed LOD of 0.2 ng/µL.

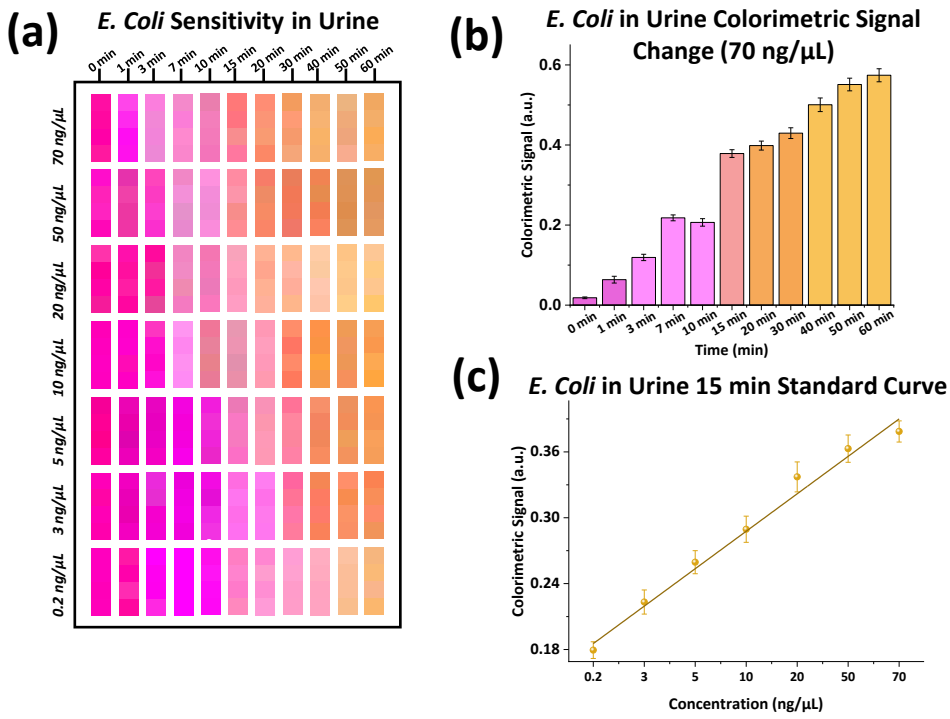

Figure 7: *E. coli* sensitivity results in urine. (a) Sampled color matrix of on-chip sensitivity test for *E. coli* in urine for 0.2 ng/µL - 70 ng/µL. (b) Quantitative colorimetric signal change for 70 ng/µL up to 60 min. Colorimetric signal changed at 3 min, passing 0.1 a.u. signal threshold. (c) Standard curve for colorimetric signal across linear range of 0.2 - 70 ng/µL, with an adjusted R^2 = 0.9868.

4.5 Discussion

In this study, we reported on a plasmonic-enhanced microfluidic biosensor integrating colorimetric LAMP for the ultra-rapid detection of bacterial DNA. The LAMP assay harnesses the pH-sensitivity of phenol red, which changes from fuchsia to yellow under acidic conditions caused by DNA amplification. Specifically, we tested this biosensor for the detection of *E. coli*, Methicillin-resistant *S. aureus*, and *P. aeruginosa* in the physiological range. Initially, we compared the difference between phenol red and resazurin in the colorimetric assay, where phenol red proved to be the favourable choice due to a faster response time and greater color contrast.

Further, we investigated the electrochemical properties of our plasmonic biosensor, finding that electron transfer into the media is enhanced in positive samples under illumination compared to negative samples and under light OFF conditions. Following this, we validated the primer sets and reaction time off-chip for each DNA sample, confirming the specificity of each primer set and reporting a visual color change in 30 min. We then determined the specificity of each primer set for the target DNA in a cross-reactivity test against non-target DNA and negative control samples. All primer sets showed 100% specificity for target DNA samples, enabling the differentiation of *E. coli*, Methicillin-resistant *S. aureus*, and *P. aeruginosa*. Sensitivity was measured in the range of 0.2 ng/µL - 70 ng/µL for *E. coli*, and between 0.2 ng/µL - 50 ng/µL for Methicillin-resistant *S. aureus* and *P. aeruginosa*, matching physiological concentrations. The color change was visible between 7-15 min for all samples, demonstrating an exceptionally rapid response time compared to PCR and culturing methods. Moreover, the biosensor demonstrated remarkable sensitivity with a calculated LOD of 1.4 ng/µL for *E. coli*, 2.2 ng/µL for Methicillin-resistant *S. aureus*, and 2.94 ng/µL for *P. aeruginosa*, which closely matched the observed LOD of 0.2 ng/µL. We further investigated the colorimetric response of *E. coli* in urine, which mimicked the response in buffer and showed a calculated LOD of 1.73 ng/µL.

Overall, our biosensor posits a strong competitive advantage compared to previously reported colorimetric biosensors for the detection of bacteria using LAMP (Table 1). Moreover, the proposed biosensor demonstrates a rapid response time and sufficiently low LOD, while providing a strong color-contrast in the colorimetric signal change. To the best of our knowledge, this biosensor is the fastest reported bacteria nucleic acid diagnostic device compared to other colorimetric biosensors. Prior to this, the fastest reported colorimetric LAMP-based diagnostic device provided a response within 60 min, whereas our device gives a response within 7-15 min.

This is a reduction in turnaround time by 8X, offering a great advantage for applications in POC settings, which often necessitate timely diagnosis of infections. In addition to this, the LOD is sufficiently low at 10 CFU or 0.2 ng/µL for *E. coli* and 0.2 ng/µL for Methicillin-resistant *S. aureus* and *P. aeruginosa*. The LOD is comparable to other reported biosensors, with the benefit of a rapid response time. Another important factor in colorimetric detection is the ability to detect the change correctly and accurately. This is aided using phenol red, as the color change from fuchsia to yellow is strikingly noticeable compared to other indicators, reported previously. We employed phenol red as an indicator that augments the optical sensitivity of the device.

Table 1: Comparison of reported colorimetric biosensors for bacteria detection using LAMP.

Bacteria	**Detection Mechanism**	**Dye**	**Limit of detection (LOD)**	**Linear Range**	**Response time**	**Reference**
		Color Change				
Salmonella	Turbidity	Precipitation	14 CFU/ml	$1.4 \times 10^1 – 1.4 \times 10^6$ CFU/mL	90 min	(53)
		Colorless → white				
E. coli, *Salmonella*, and *V. Parahaemolyticus*	Color changing dye with UV detection	Eriochrome black	100 CFU/ml	$10^2 – 10^5$ CFU/mL	60 min	(54)
		Purple → sky blue				
Salmonella	Fuchsin mediated color change	Fuchsin	3.0×10^1 CFU	$10^1 – 10^8$ CFU/mL	75 min	(55)
S. aureus		Colorless → purple	3.0×10^2 CFU	$10^2 – 10^8$ CFU/mL		
E. coli			3.0×10^1 CFU	$10^1 – 10^8$ CFU/mL		
Salmonella	Fluorescence	SYBR green dye	5000 CFU/mL in the sample or 25 RNA	$5 \times 10^3 – 5 \times 10^8$ CFU/mL	Not reported	(56)

		Dark green → fluorescent green	template/25 µL LAMP reaction cocktail			
Salmonella, *E. coli*, and *V. cholera*	Color changing dye	Calcein Yellow → green	3×10^{-5} ng/µL of bacterial DNA.	3×10^{-5} ng/µL - 3×10^{0} ng/µL	65 min	(57)
Salmonella	Color changing dye	SYBR Green I dye Light orange → yellow-green	5×10^{-3} ng/µL DNA concentration	5×10^{-3} ng/µL - 5×10^{0} ng/µL	70 min	(58)
E. coli,	Plasmonic-enhanced color changing dye	Phenol red	10 CFU/ml or 0.2 ng/µL	$10 – 10^{7}$ CFU/ml or 0.2 – 70 ng/µL	7-15 min	This work
Methicillin-resistant *S. aureus*		Fuchsia → yellow	0.2 ng/µL	0.2 – 50 ng/µL		
P. aeruginosa			0.2 ng/µL	0.2 – 50 ng/µL		

There are several unique advantages of this approach compared to other techniques. For starters, the LAMP assay is a highly specific method as it uses 4-6 primers to anneal to target DNA sites compared to PCR which uses 2 primers. Phenol red further enables sensitive detection with a strong contrast in colors compared to other indicators such as hydroxynaphthol blue, resazurin, and malachite green, which change to colors in similar hues. In addition, the plasmonic-assisted colorimetric platform allows rapid detection of the analytes due to greater optical sensitivity driven by the resonance of free electrons, which can enhance the amplification reaction. In our

application, we reduced the detection window by at least 15 min compared to off-chip results, due to the plasmonic effect. Prior studies have reported bacteria detection through colorimetric LAMP in a window of 1-2 hours (59,60). In comparison to other colorimetric approaches, our application is extraordinarily fast. As shown in Table 1, compared to other works reported in the literature, several analytical parameters including the response time and LOD have drastically improved.

In conclusion, this biosensor posits a notable alternative to standard PCR and culturing methods and paves the way forward for rapid bacterial diagnostic techniques. Moreover, this study sheds light on the value of plasmonic enhancement for optical readout techniques which employ a colorimetric approach. Future work should consider plasmonic materials to enable greater sensitivity for optical readouts. Through this work, the quantitative analysis of the amplicons was realized, positing a robust technique for colorimetric detection, and enabling integration with smart gadgets. The biosensor has also demonstrated a user-friendly interface, simple protocol, and the possibility for integration with a portable imaging technique, opening further avenues for applications in point-of-care settings. All these factors combined would facilitate rapid diagnostic and therapeutic protocols to control the spread and burden of infectious diseases driven by bacterial pathogens.

4.6 Acknowledgments

The authors thank the Faculty of Engineering at McGill University, the Natural Science and Engineering Research Council of Canada (NSERC, G247765), the Canada Foundation for Innovation (CFI, G248924), MI4 (McGill Interdisciplinary Initiative in Infection and Immunity) and New Frontiers in Research Fund (250326) for financial support.

4.7 References

1. Ho CS, Jean N, Hogan CA, Blackmon L, Jeffrey SS, Holodniy M, et al. Rapid identification of pathogenic bacteria using Raman spectroscopy and deep learning. Nat Commun 2019 101 [Internet]. 2019 Oct 30 [cited 2022 Feb 22];10(1):1–8. Available from: https://www.nature.com/articles/s41467-019-12898-9

2. Murray CJ, Ikuta KS, Sharara F, Swetschinski L, Robles Aguilar G, Gray A, et al. Global burden of bacterial antimicrobial resistance in 2019: a systematic analysis. Lancet [Internet]. 2022 Feb 12 [cited 2022 Feb 22];399(10325):629–55. Available from: http://www.thelancet.com/article/S0140673621027240/fulltext

3. Thaden JT, Park LP, Maskarinec SA, Ruffin F, Fowler VG, Van Duin D. Results from a 13-year prospective cohort study show increased mortality associated with bloodstream infections caused by pseudomonas aeruginosa compared to other bacteria. Antimicrob Agents Chemother [Internet]. 2017 Jun 1 [cited 2022 Apr 13];61(6):2671–87. Available from: https://journals.asm.org/doi/full/10.1128/AAC.02671-16

4. Poolman JT, Anderson AS. Escherichia coli and Staphylococcus aureus: leading bacterial pathogens of healthcare associated infections and bacteremia in older-age populations. https://doi.org/101080/1476058420181488590 [Internet]. 2018 Jul 3 [cited 2022 Apr 13];17(7):607–18. Available from: https://www.tandfonline.com/doi/abs/10.1080/14760584.2018.1488590

5. Reali S, Najib EY, Treuerné Balázs KE, Chern Hui Tan A, Váradi L, Hibbs DE, et al. Novel diagnostics for point-of-care bacterial detection and identification. RSC Adv [Internet]. 2019 Jul 5 [cited 2022 Feb 22];9(37):21486–97. Available from: https://pubs.rsc.org/en/content/articlehtml/2019/ra/c9ra03118a

6. Hay SI, Rao PC, Dolecek C, Day NPJ, Stergachis A, Lopez AD, et al. Measuring and mapping the global burden of antimicrobial resistance. BMC Med [Internet]. 2018 Jun 4 [cited 2022 Feb 22];16(1):1–3. Available from: https://bmcmedicine.biomedcentral.com/articles/10.1186/s12916-018-1073-z

7. Zasowski EJ, Bassetti M, Blasi F, Goossens H, Rello J, Sotgiu G, et al. A Systematic Review of the Effect of Delayed Appropriate Antibiotic Treatment on the Outcomes of Patients With Severe Bacterial Infections. Chest [Internet]. 2020 Sep 1 [cited 2022 Feb 22];158(3):929–38. Available from: https://doi.org/10.1016/j.chest.2020.03.087

8. Louie M, Louie L, Simor AE. The role of DNA amplification technology in the diagnosis of infectious diseases. CMAJ [Internet]. 2000;163(3):301–9. Available from: https://www.cmaj.ca/content/163/3/301.full

9. Oblath EA, Henley WH, Alarie JP, Ramsey JM. A microfluidic chip integrating DNA extraction and real-time PCR for the detection of bacteria in saliva. Lab Chip [Internet]. 2013 Mar 5 [cited 2022 Feb 22];13(7):1325–32. Available from: https://pubs.rsc.org/en/content/articlehtml/2013/lc/c3lc40961a

10. Pazos-Perez N, Pazos E, Catala C, Mir-Simon B, Gomez-De Pedro S, Sagales J, et al.

Ultrasensitive multiplex optical quantification of bacteria in large samples of biofluids. Sci Reports 2016 61 [Internet]. 2016 Jul 1 [cited 2022 Mar 20];6(1):1–10. Available from: https://www.nature.com/articles/srep29014

11. Wang S, Lifson MA, Inci F, Liang LG, Sheng YF, Demirci U. Advances in addressing technical challenges of point-of-care diagnostics in resource-limited settings. Expert Rev Mol Diagn [Internet]. 2016 Apr 2 [cited 2022 Mar 20];16(4):449. Available from: /pmc/articles/PMC4943866/

12. Moehling TJ, Choi G, Dugan LC, Salit M, Meagher RJ. LAMP Diagnostics at the Point-of-Care: Emerging Trends and Perspectives for the Developer Community. https://doi.org/101080/1473715920211873769 [Internet]. 2021 [cited 2022 Mar 20];21(1):43–61. Available from: https://www.tandfonline.com/doi/abs/10.1080/14737159.2021.1873769

13. Augustine R, Hasan A, Das S, Ahmed R, Mori Y, Notomi T, et al. Loop-Mediated Isothermal Amplification (LAMP): A Rapid, Sensitive, Specific, and Cost-Effective Point-of-Care Test for Coronaviruses in the Context of COVID-19 Pandemic. Biol 2020, Vol 9, Page 182 [Internet]. 2020 Jul 22 [cited 2022 Mar 20];9(8):182. Available from: https://www.mdpi.com/2079-7737/9/8/182/htm

14. Wong YP, Othman S, Lau YL, Radu S, Chee HY. Loop-mediated isothermal amplification (LAMP): a versatile technique for detection of micro-organisms. J Appl Microbiol [Internet]. 2018 Mar 1 [cited 2022 Mar 20];124(3):626–43. Available from: https://onlinelibrary.wiley.com/doi/full/10.1111/jam.13647

15. Deng MH, Zhong LY, Kamolnetr O, Limpanont Y, Lv ZY. Detection of helminths by loop-mediated isothermal amplification assay: a review of updated technology and future outlook. Infect Dis Poverty 2019 81 [Internet]. 2019 Mar 25 [cited 2022 Mar 20];8(1):1–22. Available from: https://idpjournal.biomedcentral.com/articles/10.1186/s40249-019-0530-z

16. Khan M, Wang R, Li B, Liu P, Weng Q, Chen Q. Comparative evaluation of the LAMP assay and PCR-based assays for the rapid detection of Alternaria solani. Front Microbiol. 2018 Sep 3;9(SEP):2089.

17. Soroka M, Wasowicz B, Rymaszewska A. Loop-Mediated Isothermal Amplification (LAMP): The Better Sibling of PCR? Cells 2021, Vol 10, Page 1931 [Internet]. 2021 Jul 29 [cited 2022 Apr 9];10(8):1931. Available from: https://www.mdpi.com/2073-4409/10/8/1931/htm

18. Liu Z, Yao C, Wang Y, Yang C. A G-quadruplex DNAzyme-based LAMP biosensing platform for a novel colorimetric detection of Listeria monocytogenes. Anal Methods [Internet]. 2018 Feb 22 [cited 2022 Mar 20];10(8):848–54. Available from: https://pubs.rsc.org/en/content/articlehtml/2018/ay/c7ay02908j

19. Roy S, Mohd-Naim NF, Safavieh M, Ahmed MU. Colorimetric Nucleic Acid Detection on Paper Microchip Using Loop Mediated Isothermal Amplification and Crystal Violet Dye. ACS Sensors [Internet]. 2017 Nov 22 [cited 2022 Mar 20];2(11):1713–20. Available

from: https://pubs.acs.org/doi/abs/10.1021/acssensors.7b00671

20. Oh SJ, Park BH, Choi G, Seo JH, Jung JH, Choi JS, et al. Fully automated and colorimetric foodborne pathogen detection on an integrated centrifugal microfluidic device. Lab Chip [Internet]. 2016 May 10 [cited 2022 Mar 20];16(10):1917–26. Available from: https://pubs.rsc.org/en/content/articlehtml/2016/lc/c6lc00326e

21. Kumvongpin R, Jearanaikool P, Wilailuckana C, Sae-ung N, Prasongdee P, Daduang S, et al. High sensitivity, loop-mediated isothermal amplification combined with colorimetric gold-nanoparticle probes for visual detection of high risk human papillomavirus genotypes 16 and 18. J Virol Methods. 2016 Aug 1;234:90–5.

22. Choi Y, Hyeon Hwang J, Yup Lee S, Choi Y, Hwang JH, Lee SY. Recent Trends in Nanomaterials-Based Colorimetric Detection of Pathogenic Bacteria and Viruses. Small Methods [Internet]. 2018 Apr 1 [cited 2022 Mar 21];2(4):1700351. Available from: https://onlinelibrary.wiley.com/doi/full/10.1002/smtd.201700351

23. Du J, Yu Z, Hu Z, Chen J, Zhao J, Bai Y. A low pH-based rapid and direct colorimetric sensing of bacteria using unmodified gold nanoparticles. J Microbiol Methods. 2021 Jan 1;180:106110.

24. Suebsing R, Kampeera J, Tookdee B, Withyachumnarnkul B, Turner W, Kiatpathomchai W. Evaluation of colorimetric loop-mediated isothermal amplification assay for visual detection of Streptococcus agalactiae and Streptococcus iniae in tilapia. Lett Appl Microbiol [Internet]. 2013 Oct 1 [cited 2022 Mar 21];57(4):317–24. Available from: https://onlinelibrary.wiley.com/doi/full/10.1111/lam.12114

25. Tanner NA, Zhang Y, Evans TC. Visual detection of isothermal nucleic acid amplification using pH-sensitive dyes. Biotechniques [Internet]. 2015 [cited 2021 Jun 24];58(2):59–68. Available from: www.BioTechniques.com

26. Scott AT, Layne TR, O'Connell KC, Tanner NA, Landers JP. Comparative Evaluation and Quantitative Analysis of Loop-Mediated Isothermal Amplification Indicators. Anal Chem [Internet]. 2020 Oct 6 [cited 2022 Mar 21];92(19):13343–53. Available from: https://pubs.acs.org/doi/full/10.1021/acs.analchem.0c02666

27. Nzelu CO, Cáceres AG, Guerrero-Quincho S, Tineo-Villafuerte E, Rodriquez-Delfin L, Mimori T, et al. A rapid molecular diagnosis of cutaneous leishmaniasis by colorimetric malachite green-loop-mediated isothermal amplification (LAMP) combined with an FTA card as a direct sampling tool. Acta Trop. 2016 Jan 1;153:116–9.

28. Neubrech F, Duan X, Liu N. Dynamic plasmonic color generation enabled by functional materials. Sci Adv [Internet]. 2020 Sep 1 [cited 2022 Apr 8];6(36). Available from: https://www.science.org/doi/full/10.1126/sciadv.abc2709

29. Gupta R, Kumar A, Kumar S, Pinnaka AK, Singhal NK. Naked eye colorimetric detection of Escherichia coli using aptamer conjugated graphene oxide enclosed Gold nanoparticles. Sensors Actuators B Chem. 2021 Feb 15;329:129100.

30. Amirjani A, Fatmehsari DH. Colorimetric detection of ammonia using smartphones based on localized surface plasmon resonance of silver nanoparticles. Talanta. 2018 Jan 1;176:242–6.

31. King NS, Liu L, Yang X, Cerjan B, Everitt HO, Nordlander P, et al. Fano Resonant Aluminum Nanoclusters for Plasmonic Colorimetric Sensing. ACS Nano [Internet]. 2015 Nov 24 [cited 2022 Apr 8];9(11):10628–36. Available from: https://pubs.acs.org/doi/abs/10.1021/acsnano.5b04864

32. Dyba M, Hell SW, Lukosz W. Beyond the diffraction limit? Nat 2002 4176891 [Internet]. 2002 Jun 20 [cited 2022 Apr 8];417(6891):806–7. Available from: https://www.nature.com/articles/417806a

33. Li M, Cushing SK, Wu N. Plasmon-Enhanced Optical Sensors: A Review. Analyst [Internet]. 2015 Jan 21 [cited 2022 Apr 8];140(2):386. Available from: /pmc/articles/PMC4274271/

34. Heather JM, Chain B. The sequence of sequencers: The history of sequencing DNA. Genomics. 2016 Jan 1;107(1):1–8.

35. Poole CB, Li Z, Alhassan A, Guelig D, Diesburg S, Tanner NA, et al. Colorimetric tests for diagnosis of filarial infection and vector surveillance using non-instrumented nucleic acid loop-mediated isothermal amplification (NINA-LAMP). PLoS One [Internet]. 2017 Feb 1 [cited 2022 Apr 8];12(2):e0169011. Available from: https://journals.plos.org/plosone/article?id=10.1371/journal.pone.0169011

36. Zhang Y, Lim LT. Colorimetric array indicator for NH3 and CO2 detection. Sensors Actuators B Chem. 2018 Feb 1;255:3216–26.

37. Li Z, Leustean L, Inci F, Zheng M, Demirci U, Wang S. Plasmonic-based platforms for diagnosis of infectious diseases at the point-of-care. Biotechnol Adv. 2019 Dec 1;37(8):107440.

38. Ckumdee J, Kaewphinit T, Chansiri K, Santiwatanakul S. Development of Au-nanoprobes combined with loop-mediated isothermal amplification for detection of isoniazid resistance in mycobacterium tuberculosis. J Chem. 2016;2016.

39. Nikbakht H, Gill P, Tabarraei A, Niazi A. Nanomolecular detection of human influenza virus type A using reverse transcription loop-mediated isothermal amplification assisted with rod-shaped gold nanoparticles. RSC Adv [Internet]. 2014 Mar 12 [cited 2022 Apr 8];4(26):13575–80. Available from: https://pubs.rsc.org/en/content/articlehtml/2014/ra/c3ra47398h

40. Yang KLA, Wu SY, Kwok HC, Ho HP, Kong SK. Using loop-mediated isothermal DNA amplification (LAMP) and spectral surface plasmon resonance (SPR) to detect methicillin-resistance S. aureus (MRSA). Proc - 2012 Int Conf Biomed Eng Biotechnol iCBEB 2012. 2012;647–50.

41. Hill J, Beriwal S, Chandra I, Paul VK, Kapil A, Singh T, et al. Loop-mediated isothermal

amplification assay for rapid detection of common strains of Escherichia coli. J Clin Microbiol [Internet]. 2008 Aug [cited 2021 Apr 17];46(8):2800–4. Available from: /pmc/articles/PMC2519505/

42. Chen X, Ma K, Yi X, Xiong L, Wang Y, Li S. The rapid and visual detection of methicillin-susceptible and methicillin-resistant Staphylococcus aureus using multiplex loop-mediated isothermal amplification linked to a nanoparticle-based lateral flow biosensor. Antimicrob Resist Infect Control [Internet]. 2020 Jul 17 [cited 2022 Mar 14];9(1):1–12. Available from: https://aricjournal.biomedcentral.com/articles/10.1186/s13756-020-00774-x

43. Goto M, Shimada K, Sato A, Takahashi E, Fukasawa T, Takahashi T, et al. Rapid detection of Pseudomonas aeruginosa in mouse feces by colorimetric loop-mediated isothermal amplification. J Microbiol Methods. 2010 Jun 1;81(3):247–52.

44. Desai AN, Jere A. Next-generation sequencing: ready for the clinics? Clin Genet [Internet]. 2012 Jun 1 [cited 2022 Apr 16];81(6):503–10. Available from: https://onlinelibrary.wiley.com/doi/full/10.1111/j.1399-0004.2012.01865.x

45. Underwood S, Mulvaney P. Effect of the Solution Refractive Index on the Color of Gold Colloids. Langmuir [Internet]. 1994 Oct 1 [cited 2022 Apr 16];10(10):3427–30. Available from: https://pubs.acs.org/doi/abs/10.1021/la00022a011

46. Moyer R 54, Campbell JJR. M]~CHANISM OF RESAZURIN REDUCTION IN MILK OF LOW BACTERIAL CONTENT. J Dairy Sci. 46:897–906.

47. Zare M, Amin MM, Nikaeen M, Bina B, Pourzamani H, Fatehizadeh A, et al. Resazurin reduction assay, a useful tool for assessment of heavy metal toxicity in acidic conditions. Environ Monit Assess [Internet]. 2015 May 1 [cited 2022 Jun 19];187(5):1–11. Available from: https://link.springer.com/article/10.1007/s10661-015-4392-y

48. Mauriz E. Clinical Applications of Visual Plasmonic Colorimetric Sensing. Sensors (Basel) [Internet]. 2020 Nov 1 [cited 2022 Jun 27];20(21):1–31. Available from: /pmc/articles/PMC7663786/

49. Rao VG, Aslam U, Linic S. Chemical Requirement for Extracting Energetic Charge Carriers from Plasmonic Metal Nanoparticles to Perform Electron-Transfer Reactions. J Am Chem Soc [Internet]. 2019 Jan 9 [cited 2022 Jun 27];141(1):643–7. Available from: https://pubs.acs.org/doi/abs/10.1021/jacs.8b11949

50. Ogu GI, Ezeadila JO, Echetabu IE, Ogu GI, Aneke FA. Isolation, Identification and Antibiotic Sensitivity Pattern of Bacteria from Urine Samples of Female Students L... Original Research Article Isolation, Identification and Antibiotic Sensitivity Pattern of Bacteria from Urine Samples of Female Students Living in the Hostels of Chukwuemeka Odumegwu Ojukwu University, Uli Campus, Anambra State, Nigeria. IntJCurrMicrobiolAppSci [Internet]. 2015 [cited 2022 Apr 18];4(12):255–62. Available from: http://www.ijcmas.com

51. Saad Abdulsahib S. Identification of the respiratory tract infection due to methicillin-

resistant Staphylococcus aureus by TaqMan real-time PCR. Abdulsahib Med J Cell Biol [Internet]. 2021 [cited 2022 Apr 18]; Available from: www.ncbi.nlm.nih.gov/gene/

52. Mangiaterra G, Amiri M, Di Cesare A, Pasquaroli S, Manso E, Cirilli N, et al. Detection of viable but non-culturable Pseudomonas aeruginosa in cystic fibrosis by qPCR: a validation study. BMC Infect Dis [Internet]. 2018 Dec 27 [cited 2022 Apr 18];18(1). Available from: /pmc/articles/PMC6307279/

53. Wang S, Liu N, Zheng L, Cai G, Lin J. A lab-on-chip device for the sample-in-result-out detection of viable: Salmonella using loop-mediated isothermal amplification and real-time turbidity monitoring. Lab Chip [Internet]. 2020 Jul 7 [cited 2021 Jan 15];20(13):2296–305. Available from: https://pubs.rsc.org/en/content/articlehtml/2020/lc/d0lc00290a

54. Nguyen H Van, Nguyen VD, Lee EY, Seo TS. Point-of-care genetic analysis for multiplex pathogenic bacteria on a fully integrated centrifugal microdevice with a large-volume sample. Biosens Bioelectron. 2019 Jul 1;136:132–9.

55. Trinh KTL, Trinh TND, Lee NY. Fully integrated and slidable paper-embedded plastic microdevice for point-of-care testing of multiple foodborne pathogens. Biosens Bioelectron. 2019 Jun 15;135:120–8.

56. Azizi M, Zaferani M, Cheong SH, Abbaspourrad A. Pathogenic Bacteria Detection Using RNA-Based Loop-Mediated Isothermal-Amplification-Assisted Nucleic Acid Amplification via Droplet Microfluidics. ACS Sensors [Internet]. 2019 Apr 26 [cited 2021 Jan 12];4(4):841–8. Available from: https://pubs.acs.org/sharingguidelines

57. Sayad A, Ibrahim F, Mukim Uddin S, Cho J, Madou M, Thong KL. A microdevice for rapid, monoplex and colorimetric detection of foodborne pathogens using a centrifugal microfluidic platform. Biosens Bioelectron. 2018 Feb 15;100:96–104.

58. Sayad AA, Ibrahim F, Uddin SM, Pei KX, Mohktar MS, Madou M, et al. A microfluidic lab-on-a-disc integrated loop mediated isothermal amplification for foodborne pathogen detection. Sensors Actuators, B Chem. 2016 May 1;227:600–9.

59. Jaroenram W, Cecere P, Pompa PP. Xylenol orange-based loop-mediated DNA isothermal amplification for sensitive naked-eye detection of Escherichia coli. J Microbiol Methods. 2019 Jan 1;156:9–14.

60. Safavieh M, Ahmed MU, Sokullu E, Ng A, Zourob M. A simple cassette as point-of-care diagnostic device for naked-eye colorimetric bacteria detection. Analyst [Internet]. 2013 Dec 9 [cited 2022 Apr 21];139(2):482–7. Available from: https://pubs.rsc.org/en/content/articlehtml/2014/an/c3an01859h

4.8 Supplementary Information

Table S1: Primer sets and initial concentration of each primer for *E. coli*, Methicillin-resistant *S. aureus*, and *P. aeruginosa*.

***E. Coli* LAMP Primer Set Targeting *malB* Gene**		
Primer	**5' to 3' Sequence**	**Initial Concentration**
F3	GCCATCTCCTGATGACGC	0.2 µM
B3	ATTTACCGCAGCCAGACG	0.2 µM
FIP	CATTTTGCAGCTGTACGCTCGCAGCCCATCAT GAATGTTGCT	1.6 µM
BIP	CTGGGGCGAGGTCGTGGTATTCCGACAAACAC CACGAATT	1.6 µM
LF	CTTTGTAACAACCTGTCATCGACA	0.8 µM
LB	ATCAATCTCGATATCCATGAAGGTG	0.8 µM
Methicillin-resistant *S. Aureus* LAMP Primer Set Targeting *mecA* Gene		
Primer	**5' to 3' Sequence**	**Initial Concentration**
F3	GGCTCAGGTACTGCTATC	0.4 µM
B3	TTGTTATTTAACCCAATCATTGC	0.4 µM
FIP	ATGCCATACATAAATGGATAGACGTCAAACAG GTGAATTATTAGCACTT	1.6 µM
BIP	CCGAAGATAAAAAAGAACCTCTGCTTTTTTGA GTTGAACCTGGTG	1.6 µM
LF	CATATGAAGGTGTGCTTAC	0.8 µM
LB	CAAGTTCCAGATTACAACTT	0.8 µM
***P. Aeruginosa* LAMP Primer Set Targeting *oprL* Gene**		
Primer	**5' to 3' Sequence**	**Initial Concentration**
F3	GCGTTGCCGCCAACAATG	0.2 µM
B3	CATGCGGGCAACCTCTC	0.2 µM
FIP	GTTGTCACCCCACCTCCGGGCGGCAACGTTCC TCC	1.6 µM
BIP	CTCCGTGCAGGGCGAACTGCAGGCGAGCCAAC TC	1.6 µM
LF	ACCTGCCGTGCCATACC	0.8 µM
LB	GTTCATGCAGCTCCAGCAG	0.8 µM

4.8.1 Supplementary Note 1: Fabrication of Microfluidic Biosensor

In the fabrication of the biosensor, we followed a three-step photolithography protocol. Briefly, features of the heater element were first patterned in an AZ 9245 (10µm) positive

photoresist layer on a 6-inch silicon wafer (Figure S1a). Next, a buffered oxide etch (BOE) process was used to embed the features onto a silicon substrate, while removing the original oxide layer on top of the silicon. We selectively removed the silicon substrate through a potassium hydroxide (KOH) etch step (Figure S1a). A lift-off process enabled the selective deposition of aluminum in the etched features which included a second lithography step using an S1813 positive photoresist (2.14 µm) and electron-beam evaporation of 240 nm of aluminum (BJD 1600, rate 1 $Å.s^{-1}$) (Figure S1b). We removed remaining aluminum by immersing the wafer in a fitting solution (Remover1165), which removed the S1813 photoresist layer (Figure S1b). In the third lithography step, we fabricated the fluidic channels and chambers in a 50 µm thick SU-8 layer (Figure S1c). In order to generate the colorimetric platform, we developed a colloidal self-assembled monolayer (SAM) of polystyrene nanobeads at an air-water interface and the resulting lattice was transferred to the colorimetric readout window of the device (Figure S1d). A 120 nm zinc-oxide film was deposited as a back-reflector and a thin aluminum layer was deposited as the plasmonic surface (Figure S1d). This provided a color-tunable window with a white background enabled by surface plasmon resonance. Lastly, a polydimethylsiloxane (PDMS SYLGARD 184 silicone elastomer, Dow Consumer Solutions, QC, Canada) layer was bonded to individual chips to create the resulting biosensor (Figure S1e). In this process, a PDMS elastomer was homogenized with a curing agent in a 10:1 ratio by weight, degassed in a desiccator, and left to cure at 65^{o}C overnight. After this, the PDMS was treated with air plasma for 60 s and bonded to the SU8 coated chip, which was incubated overnight at 105 ^{o}C.

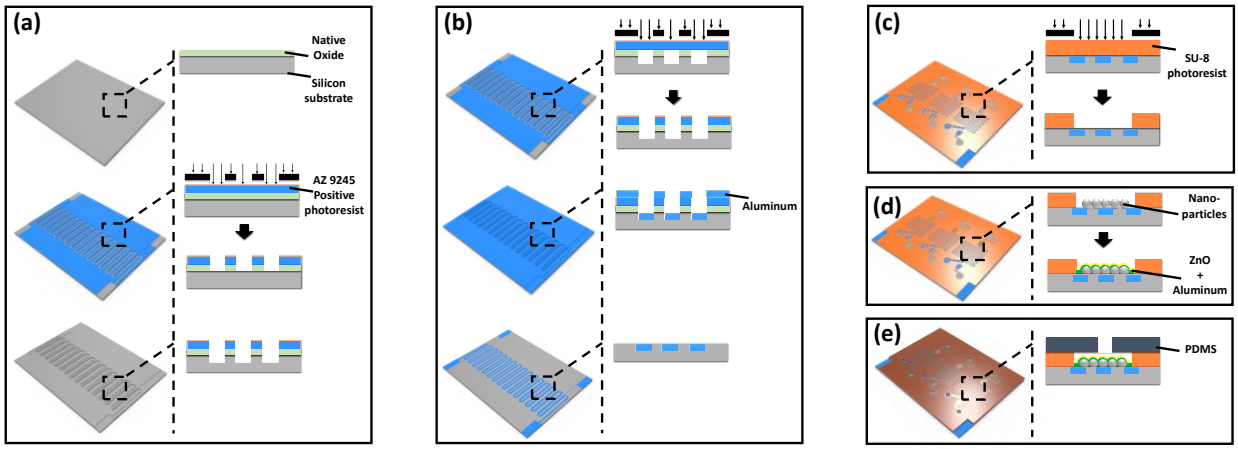

Figure S1: Fabrication protocol of microfluidic biosensor; isometric view (left panel), cross-section (right panel). (a) Initial lithography step for etching of electrode features on a silicon wafer. (b) Second lithography step, a lift-off process, for selective deposition of aluminum in etched features. (c) Final lithography step for printing fluidic components and features on an SU-8 negative photoresist layer. (d) Fabrication of nanoparticles in colorimetric platform followed by e-beam evaporation of ZnO and Al films, creating plasmonic surface. (e) PDMS bonding with microfluidic biosensor to seal fluidic features.

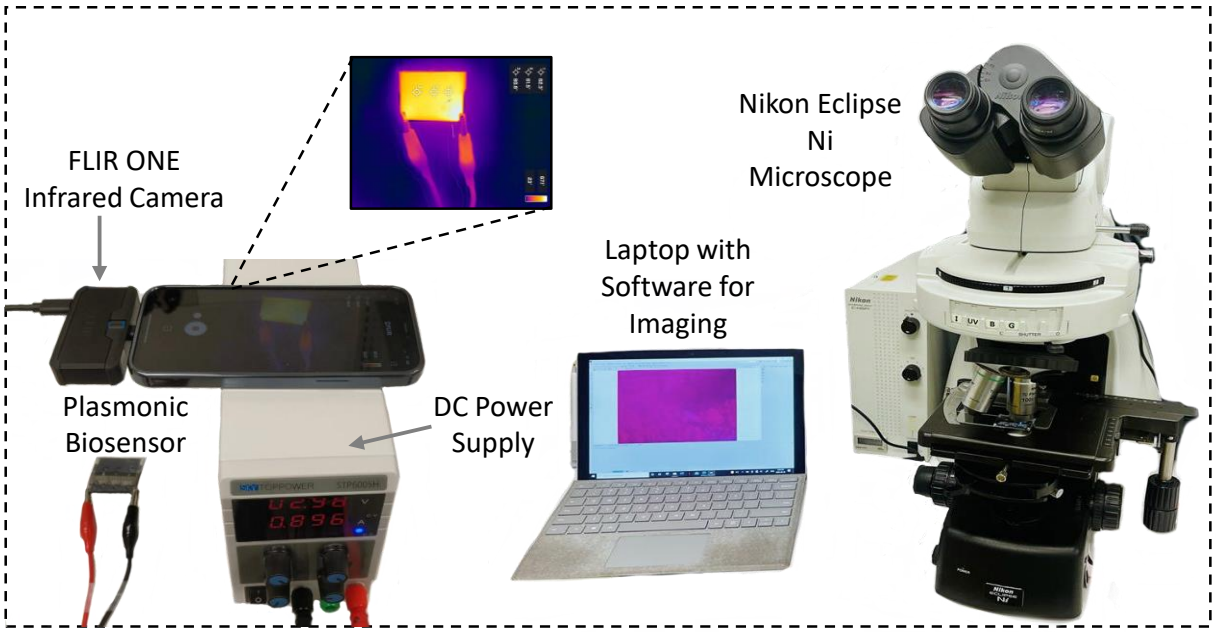

Figure S2: Complete set-up of work-flow. Microfluidic biosensor is connected to DC power supply for heating. FLIR One infrared camera is connected to smartphone to monitor changes in reaction temperature in colorimetric chambers. Biosensor is placed under Nikon microscope and color changes are visualized using camera and imaging software on laptop.

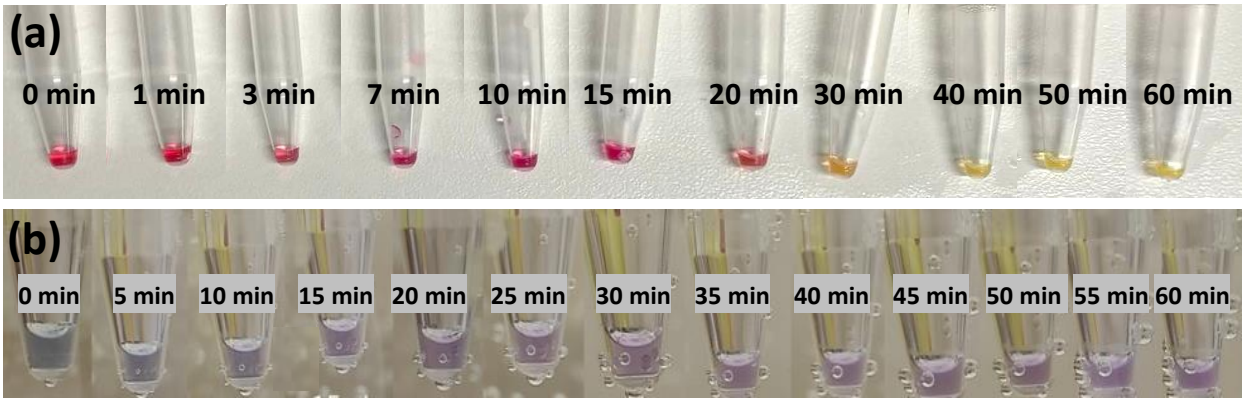

Figure S3: Off-chip assay results of phenol red and resazurin. (a) Images of phenol red assay, where visible color change was observed at 30 min. (b) Images of resazurin assay, where visible color change was observed at 35 min.

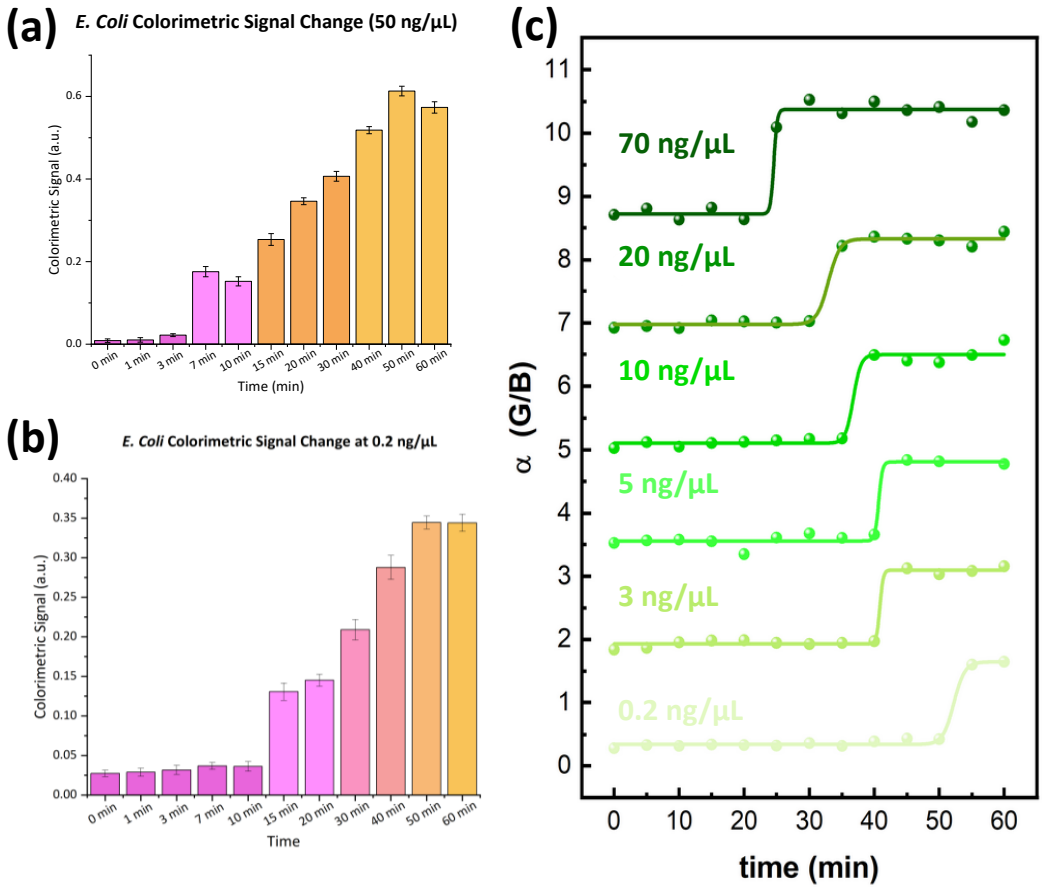

Figure S4: Comparison of quantitative colorimetric signal between phenol red and resazurin assays in biosensor/platform. (a) Colorimetric signal change at 50 ng/µL of *E. coli* DNA; signal spikes at 7 min. (b) Colorimetric signal change at 0.2 ng/µL of *E. coli* DNA; signal spikes at 15 min. (c) Quantitative colorimetric signal for resazurin experiments with *E. coli* DNA. Signal change evident by spike in α value for given concentrations.

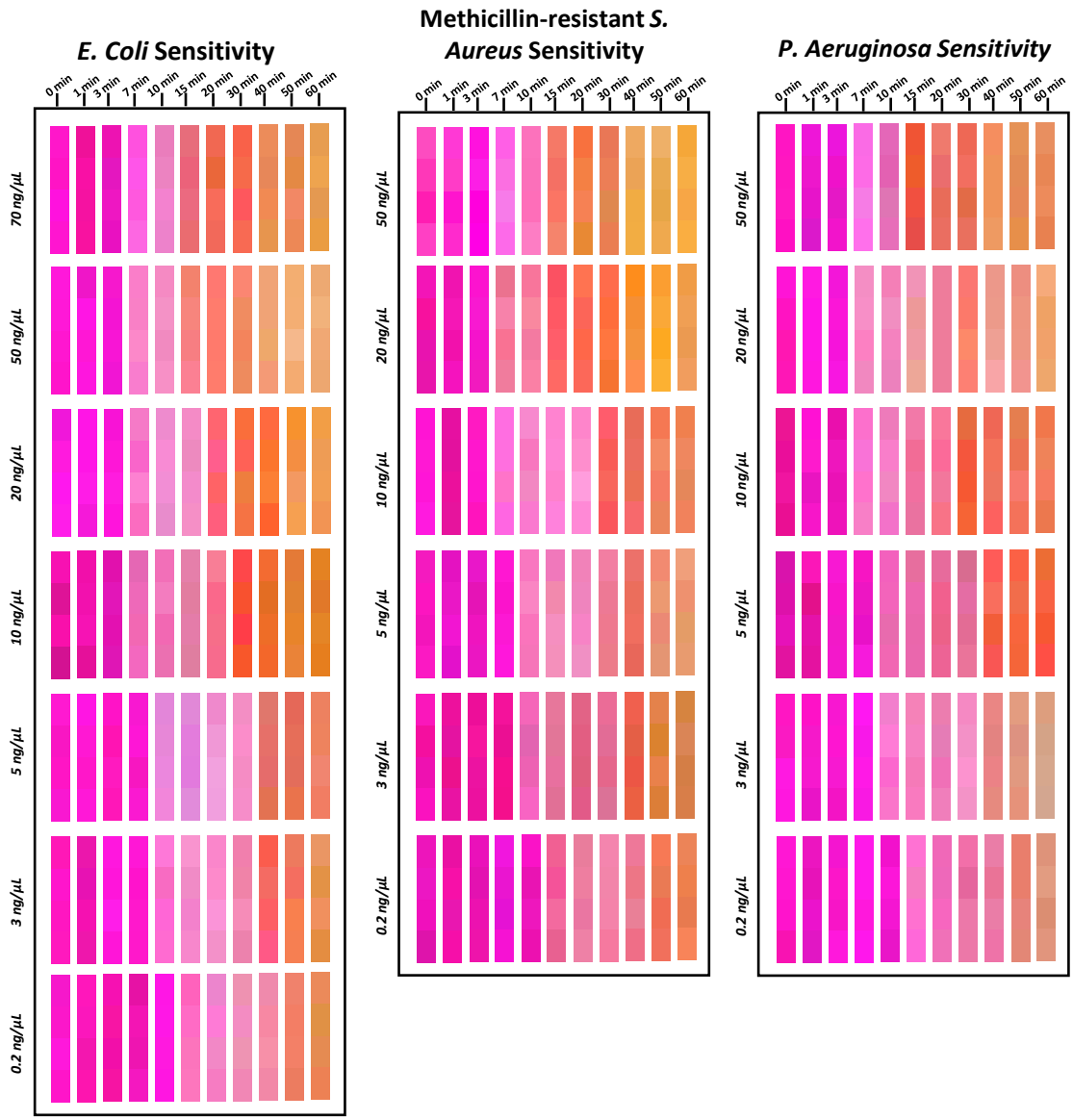

Figure S5: Complete sampled color matrix of on-chip sensitivity test for *E. coli*, Methicillin-resistant *S. aureus*, and *P. aeruginosa*.

5 General Discussion

5.1 Summary

In Chapter 2, I first introduced the threat of infectious diseases driven by bacteria and the need for POC biosensors for effectively combatting bacterial infections in a timely manner. I then reviewed the relevant works revolving around recent published colorimetric biosensors for the detection of bacteria. These included both nucleic acid and immunoassay-based biosensors. From published works, the average time to results were ~90 min for colorimetric biosensors, which is a stark contrast to the average time of standard diagnostic tests such as culturing and PCR which can take up to 72 hours in many cases. Moreover, the reported LOD was in some cases, even more sensitive than traditional approaches. These features can be attributed to the scaled downsizes and small reaction volumes required, further supporting these novel biosensors as excellent substitutes for standard approaches.

Despite the notable progress made in recent years, one of the biggest challenges that remains with colorimetric approaches is the optical sensitivity of the sensor, which can hinder reaction times and lead to false-positive/negative results. A way that researchers have addressed this issue is by employing plasmonic nanomaterials which provide high color tunability across the visible spectrum. This has enabled researchers to accurately detect samples in a fast response time while ensuring sensitive detection of bacteria.

In Chapter 3, I presented the optimization of the study presented in Chapter 4. Particularly, we optimized the primer set, DNA extraction protocol, and concentration of resazurin. This allowed us to achieve stronger data while ensuring high sensitivity, specificity, and faster results.

Moreover, these optimization steps allowed us to ensure that this biosensor would translate well in POC settings.

Plasmonic nanomaterials were at the centre of our work as described in the manuscript presented in Chapter 4, which discussed a novel microfluidic biosensor for the colorimetric detection of three types of bacteria: *E. coli*, Methicillin-resistant *S. aureus*, and *P. aeruginosa*, within 7 min. Our biosensor combines an on-chip LAMP assay, integrated heater element, and colorimetric plasmonic-enhanced readout window for the sensitive and rapid detection of bacterial DNA. We presented a study which first presented the properties of the microfluidic biosensor, namely the plasmonic colorimetric platform and workflow. Next, we evaluated two colorimetric dyes, phenol red and resazurin, in a LAMP assay and determined that phenol red was the most suitable option for a stark color contrast and fast response. We also explored the electrochemical properties of the biosensor, finding that electron transfer from the plasmonic surface is highest for positive samples under light illumination, and that electrons play a key role in enhancing the colorimetric response. Following this, we investigated the off-chip response of the LAMP assay for each bacteria primer set, showing results within 30 min. In a cross-reactivity test, we determined the specificity for each primer using the biosensor, demonstrating that each primer set was specific only for target DNA and thus exhibited 100% specificity. Sensitivity experiments showed that the DNA could be detected in a linear range between 0.2 ng/µL - 50 ng/µL, with the detection time ranging between 7 min and 15 min for all samples. The LOD was experimentally determined to be 0.2 ng/µL, closely matching the calculated LOD for each DNA sample. Moreover, we tested the sensitivity of the biosensor in measuring *E. coli* DNA samples in urine, which demonstrated an LOD of 0.2 ng/µL, and linearity between 0.2 ng/µL - 70 ng/µL, with an extraordinary detection time between 3-15 min.

Overall, this biosensor posits several advantages including a rapid response time and sufficiently low LOD, while employing a colorimetric signal change with a dramatic color contrast, enabling sensitive detection. This biosensor proposes a strong alternative to standard PCR and culturing approaches while paving the way for rapid bacterial diagnostic techniques, highlighting the value and importance of plasmonic materials in sensitive detection of analytes.

5.2 Contribution to Field

The work in Chapter 4, considerably contributes to the field of plasmonic nano sensing for the detection of infectious diseases driven by bacteria for several reasons. First, to the best of our knowledge, this biosensor is the fastest reported bacteria diagnostic device compared to reported biosensors with a response time of 7-15 min. In particular, from the nucleic acid-based biosensors captured in Chapter 2, the fastest reported response time was 40 min and from the immunoassay-based biosensors, the fastest response time was 35 min. When comparing LAMP-based colorimetric biosensors, reported in Chapter 4, our biosensor is 8X faster, which is a stark difference. This is particularly important for applications in POC settings, which often require timely diagnosis of infections to effectively combat disease outbreaks.

Another unique aspect of this biosensor compared to other published works is the plasmonic color-sensitive platform combined with phenol red, which led to a high color contrast, and enabled highly sensitive detection of samples. As demonstrated by previous works, plasmonic materials are particularly valuable in enabling enhanced optical sensitivity in colorimetric assays across the visible spectrum. In our approach, we combined aluminum coated nanostructures and a zinc-oxide back reflector with a phenol red colorimetric assay. This approach further supported the effect of plasmonic nanomaterials in enhancing optical sensitivity of biological assays, as the

off-chip response of the phenol red assay was 30 min, and the on-chip response was between 7-15 min. Notably, phenol red is distinctive compared to other color changing dyes as the color change from fuchsia to yellow is a strong color contrast. Other indicators often change colors within similar hues such as light orange to yellow, yellow to green, and purple to blue. This makes it difficult to distinguish color changes, as the human eye is insensitive to low level color contrasts. Therefore, phenol red stands out as an exceptional color changing agent for monitoring nucleic acid amplification due to its striking color change.

Finally, we observed 100% specificity for each of the primer sets used. This in large part is due to the number of primers used in the LAMP assay and inherent specificity of genetic sequence detection in LAMP compared to immunoassay-based approaches. Our study further validates LAMP as a strong tool for nucleic acid amplification, especially for applications in POC settings where it may be used as a substitute for standard PCR tests.

In general, the response time, sensitivity enabled by the plasmonic-enhanced nanostructures, and specificity of the LAMP assay support this method as a robust technique for bacteria diagnosis. This study may advise future studies in designing highly sensitive nucleic acid detection approaches for timely applications in POC settings. Furthermore, this study further highlights the importance and value of plasmonic materials as well as LAMP. Future studies should strongly consider these approaches for boosting detection.

5.3 Limitations of Presented Work

There are some components of this study that limit the application of our biosensor as a stand-alone device at the POC. In particular, this study used a Nikon brightfield bench-top microscope for imaging and DC power supply for heating. Evidently remote, isolated and low-

resource settings may not have access to these technologies, due to their high cost and lack of portability. However, it is necessary to note that we have demonstrated full POC capability of this approach in another prepared work where we employed a fully automated, stand-alone version of this biosensor, dubbed QolorEx, in the detection of viral nucleic acids. In our QolorEx study, we combined the microfluidic device with a portable imaging box and smartphone app for complete automation of this biosensor.

5.4 Future Directions for Point-of-Care Colorimetric Biosensors

Point-of-care biosensors have made remarkable progress, especially in the past decade. Future efforts ought to focus on the translation of fundamental research into the clinic and home. This endeavour will require the coordinated collaboration between multiple stakeholders including front-line medical staff, scientists, engineers, patients, production companies, and end-users. Another key consideration is the need for high volume manufacturing, while maintaining quality standards to achieve commercial success. Due to the multidisciplinary nature of colorimetric-based biosensors, a unified effort is required from all parties involved for the successful commercialization of devices.

In the effort to commercialize such devices, integration and standardization are imperative. It is critical to maintain high quality standards among fabricated devices that are produced in masses. Otherwise, variability in devices can lead to unreproducible results, affecting end-users. In addition, greater emphasis needs to be placed on the integration of all steps of detection from end-to-end, including sample loading, extraction, amplification, and analysis. This enables user-friendliness that is a key aspect of POC detection. The opportunities for the development and application of colorimetric biosensors are endless. With great anticipation, we expect the growth

and expansion of colorimetric biosensors from proof-of-concept experiments to commercial, real-world applications, particularly in point-of-care settings.

6 Final Conclusion & Summary

In this thesis I presented a manuscript on the colorimetric detection of bacterial DNA using a plasmonic-enhanced biosensor. The five objectives of this research were fulfilled in a series of experiments which included determining the preferrable color-changing dye, investigating the electrochemical properties, testing the specificity of the primers, sensitivity of the device, and assessing the response of the device in simulated patient samples. We determined that phenol red was the preferrable dye and that positive samples under illumination received greatest electron transfer from the plasmonic surface. Each primer set was specific only for target DNA and thus exhibited 100% specificity. Next, sensitivity experiments showed that the DNA could be detected in a linear range between 0.2 ng/µL - 50 ng/µL, with a detection time as early as 7 min. The experimental LOD was determined to be 0.2 ng/µL, closely matching the calculated LOD for each DNA concentration. Finally, we tested the sensitivity of the biosensor in detecting *E. coli* DNA samples in urine, which demonstrated an LOD of 0.2 ng/µL, and linearity between 0.2 ng/µL - 70 ng/µL, with an extraordinary detection time between 3-15 min. This work supports our initial hypothesis, as this biosensor successfully detected samples in a much faster rate compared to standard diagnostic tests. Moreover, this biosensor can easily be translated to point-of-care settings due to its user-friendly interface, portability, and simple operation protocol.

Moving foreword, greater emphasis should be placed on plasmonic materials for enhancing colorimetric detection, due to their supreme optical sensitivity. In addition, it is imperative for the diagnostics community to streamline efforts across multiple stakeholders in an effort to commercialize devices. Integration and standardization of devices are two factors that are paramount for the transition from benchtop devices to applications in point-of-care settings, which will ultimately help combat the fight against infectious bacterial pathogens.

Master Bibliography

1. Serwecińska L. Antimicrobials and Antibiotic-Resistant Bacteria: A Risk to the Environment and to Public Health. Water 2020, Vol 12, Page 3313 [Internet]. 2020 Nov 25 [cited 2022 May 19];12(12):3313. Available from: https://www.mdpi.com/2073-4441/12/12/3313/htm

2. Stilianakis NI, Drossinos Y. Dynamics of infectious disease transmission by inhalable respiratory droplets. J R Soc Interface [Internet]. 2010 Sep 6 [cited 2022 May 19];7(50):1355–66. Available from: https://royalsocietypublishing.org/doi/full/10.1098/rsif.2010.0026

3. Salathé M, Kazandjieva M, Lee JW, Levis P, Feldman MW, Jones JH. A high-resolution human contact network for infectious disease transmission. Proc Natl Acad Sci U S A [Internet]. 2010 Dec 21 [cited 2022 May 19];107(51):22020–5. Available from: www.pnas.org/cgi/doi/10.1073/pnas.1009094108

4. Stoddard ST, Morrison AC, Vazquez-Prokopec GM, Soldan VP, Kochel TJ, Kitron U, et al. The Role of Human Movement in the Transmission of Vector-Borne Pathogens. PLoS Negl Trop Dis [Internet]. 2009 Jul [cited 2022 May 19];3(7):e481. Available from: https://journals.plos.org/plosntds/article?id=10.1371/journal.pntd.0000481

5. Park JY, Seo KS. Staphylococcus Aureus. Food Microbiol Fundam Front [Internet]. 2022 Feb 14 [cited 2022 May 19];555–84. Available from: https://www.ncbi.nlm.nih.gov/books/NBK441868/

6. The top 10 causes of death [Internet]. World Health Organization. 2020 [cited 2022 May 19]. Available from: https://www.who.int/news-room/fact-sheets/detail/the-top-10-causes-of-death

7. Doron S, Gorbach SL. Bacterial Infections: Overview. Int Encycl Public Heal [Internet]. 2008 [cited 2022 May 19];273. Available from: /pmc/articles/PMC7149789/

8. Kim C, Holm M, Frost I, Hasso-Agopsowicz M, Abbas K. Global and regional burden of attributable and associated bacterial antimicrobial resistance avertable by vaccination: modelling study. medRxiv [Internet]. 2022 May 10 [cited 2022 May 19];2022.05.08.22274821. Available from: https://www.medrxiv.org/content/10.1101/2022.05.08.22274821v1

9. Proulx N, Fréchette D, Toye B, Chan J, Kravcik S. Delays in the administration of antibiotics are associated with mortality from adult acute bacterial meningitis. QJM An Int J Med [Internet]. 2005 Apr 1 [cited 2022 May 20];98(4):291–8. Available from: https://academic.oup.com/qjmed/article/98/4/291/1558829

10. Peebles K, Velloza J, Balkus JE, McClelland RS, Barnabas R V. High Global Burden and Costs of Bacterial Vaginosis: A Systematic Review and Meta-Analysis. Sex Transm Dis [Internet]. 2019 May 1 [cited 2022 May 20];46(5):304–11. Available from: https://journals.lww.com/stdjournal/Fulltext/2019/05000/High_Global_Burden_and_Costs

_of_Bacterial.5.aspx

11. Sharma S, Zapatero-Rodríguez J, Estrela P, O'Kennedy R. Point-of-Care Diagnostics in Low Resource Settings: Present Status and Future Role of Microfluidics. Biosens 2015, Vol 5, Pages 577-601 [Internet]. 2015 Aug 13 [cited 2022 May 20];5(3):577–601. Available from: https://www.mdpi.com/2079-6374/5/3/577/htm

12. World Health Organization W. New report calls for urgent action to avert antimicrobial resistance crisis [Internet]. 2019 [cited 2022 May 20]. Available from: https://www.who.int/news/item/29-04-2019-new-report-calls-for-urgent-action-to-avert-antimicrobial-resistance-crisis

13. Váradi L, Luo JL, Hibbs DE, Perry JD, Anderson RJ, Orenga S, et al. Methods for the detection and identification of pathogenic bacteria: past, present, and future. Chem Soc Rev [Internet]. 2017 Aug 14 [cited 2022 May 20];46(16):4818–32. Available from: https://pubs.rsc.org/en/content/articlehtml/2017/cs/c6cs00693k

14. Iskandar K, Molinier L, Hallit S, Sartelli M, Hardcastle TC, Haque M, et al. Surveillance of antimicrobial resistance in low- and middle-income countries: a scattered picture. Antimicrob Resist Infect Control 2021 101 [Internet]. 2021 Mar 31 [cited 2022 May 20];10(1):1–19. Available from: https://aricjournal.biomedcentral.com/articles/10.1186/s13756-021-00931-w

15. Babaie P, Saadati A, Hasanzadeh M. Recent progress and challenges on the bioassay of pathogenic bacteria. J Biomed Mater Res Part B Appl Biomater [Internet]. 2021 Apr 1 [cited 2022 May 20];109(4):548–71. Available from: https://onlinelibrary.wiley.com/doi/full/10.1002/jbm.b.34723

16. Humphries RM, Ambler J, Mitchell SL, Castanheira M, Dingle T, Hindler JA, et al. CLSI methods development and standardization working group best practices for evaluation of antimicrobial susceptibility tests [Internet]. Vol. 56, Journal of Clinical Microbiology. American Society for Microbiology; 2018 [cited 2021 Feb 14]. Available from: https://pubmed.ncbi.nlm.nih.gov/29367292/

17. Siopi M, Pournaras S, Meletiadis J. Comparative evaluation of sensititre YeastOne and CLSI M38-A2 reference method for antifungal susceptibility testing of Aspergillus spp. against echinocandins. J Clin Microbiol [Internet]. 2017 Jun 1 [cited 2021 Feb 14];55(6):1714–9. Available from: https://doi.org/10

18. Vouga M, Greub G. Emerging bacterial pathogens: The past and beyond [Internet]. Vol. 22, Clinical Microbiology and Infection. Elsevier B.V.; 2016 [cited 2021 Feb 14]. p. 12–21. Available from: http://dx.doi.org/10.1016/j.cmi.2015.10.010

19. Andrews JR, Ryan ET. Diagnostics for invasive Salmonella infections: Current challenges and future directions. Vol. 33, Vaccine. Elsevier Ltd; 2015. p. C8–15.

20. Sudhaharan S, Vanjari L, Mamidi N, Ede N, Vemu L. Evaluation of LAMP assay using phenotypic tests and conventional PCR for detection of nuc and mecA genes among clinical isolates of staphylococcus SPP. J Clin Diagnostic Res [Internet]. 2015 Aug 1

[cited 2021 Jun 28];9(8):DC06–9. Available from: /pmc/articles/PMC4576532/

21. Tan X, Khaing Oo MK, Gong Y, Li Y, Zhu H, Fan X. Glass capillary based microfluidic ELISA for rapid diagnostics. Analyst [Internet]. 2017 Jul 7 [cited 2021 Jun 28];142(13):2378–85. Available from: https://pubs.rsc.org/en/content/articlehtml/2017/an/c7an00523g

22. Raeymaekers L. Basic principles of quantitative PCR. Appl Biochem Biotechnol - Part B Mol Biotechnol [Internet]. 2000 [cited 2021 Mar 4];15(2):115–22. Available from: https://link.springer.com/article/10.1385/MB:15:2:115

23. Brinati D, Campagner A, Ferrari D, Locatelli M, Banfi G, Cabitza F. Detection of COVID-19 Infection from Routine Blood Exams with Machine Learning: A Feasibility Study. J Med Syst [Internet]. 2020 Aug 1 [cited 2021 Mar 10];44(8):1–12. Available from: https://doi.org/10.1007/s10916-020-01597-4

24. Cherpillod P, Schibler M, Vieille G, Cordey S, Mamin A, Vetter P, et al. Ebola virus disease diagnosis by real-time RT-PCR: A comparative study of 11 different procedures. J Clin Virol. 2016 Apr 1;77:9–14.

25. Athamanolap P, Hsieh K, Chen L, Yang S, Wang TH. Integrated Bacterial Identification and Antimicrobial Susceptibility Testing Using PCR and High-Resolution Melt. Anal Chem [Internet]. 2017 Nov 7 [cited 2021 Feb 21];89(21):11529–36. Available from: https://pubs.acs.org/sharingguidelines

26. Huang HS, Tsai CL, Chang J, Hsu TC, Lin S, Lee CC. Multiplex PCR system for the rapid diagnosis of respiratory virus infection: systematic review and meta-analysis. Vol. 24, Clinical Microbiology and Infection. Elsevier B.V.; 2018. p. 1055–63.

27. Kashir J, Yaqinuddin A. Loop mediated isothermal amplification (LAMP) assays as a rapid diagnostic for COVID-19. Med Hypotheses [Internet]. 2020 Aug 1 [cited 2021 Jun 28];141:109786. Available from: /pmc/articles/PMC7182526/

28. Zanoli LM, Spoto G. Isothermal amplification methods for the detection of nucleic acids in microfluidic devices [Internet]. Vol. 3, Biosensors. MDPI AG; 2013 [cited 2021 Jun 22]. p. 18–43. Available from: /pmc/articles/PMC4263587/

29. Chen A, Yang S. Replacing antibodies with aptamers in lateral flow immunoassay. Vol. 71, Biosensors and Bioelectronics. Elsevier Ltd; 2015. p. 230–42.

30. Lequin RM. Enzyme Immunoassay (EIA)/Enzyme-Linked Immunosorbent Assay (ELISA). Clin Chem [Internet]. 2005 Dec 1 [cited 2021 Feb 28];51(12):2415–8. Available from: https://academic.oup.com/clinchem/article/51/12/2415/5629720

31. Hoffmann B, Beer M, Reid SM, Mertens P, Oura CAL, van Rijn PA, et al. A review of RT-PCR technologies used in veterinary virology and disease control: Sensitive and specific diagnosis of five livestock diseases notifiable to the World Organisation for Animal Health. Vol. 139, Veterinary Microbiology. Elsevier; 2009. p. 1–23.

32. Rijsman LH, Monkelbaan JF, Kusters JG. Clinical consequences of polymerase chain

reaction-based diagnosis of intestinal parasitic infections. J Gastroenterol Hepatol [Internet]. 2016 Nov 1 [cited 2021 Feb 21];31(11):1808–15. Available from: http://doi.wiley.com/10.1111/jgh.13412

33. Yang S, Rothman RE. PCR-based diagnostics for infectious diseases: Uses, limitations, and future applications in acute-care settings. Vol. 4, Lancet Infectious Diseases. Elsevier; 2004. p. 337–48.

34. Louie M, Louie L, Simor AE. The role of DNA amplification technology in the diagnosis of infectious diseases. CMAJ [Internet]. 2000;163(3):301–9. Available from: https://www.cmaj.ca/content/163/3/301.full

35. Sakamoto S, Putalun W, Vimolmangkang S, Phoolcharoen W, Shoyama Y, Tanaka H, et al. Enzyme-linked immunosorbent assay for the quantitative/qualitative analysis of plant secondary metabolites [Internet]. Vol. 72, Journal of Natural Medicines. Springer Tokyo; 2018 [cited 2021 Feb 22]. p. 32–42. Available from: /pmc/articles/PMC5775980/

36. Heidt B, Siqueira WF, Eersels K, Diliën H, Van Grinsven B, Fujiwara RT, et al. Point of Care Diagnostics in Resource-Limited Settings: A Review of the Present and Future of PoC in Its Most Needed Environment. Biosens 2020, Vol 10, Page 133 [Internet]. 2020 Sep 24 [cited 2022 May 20];10(10):133. Available from: https://www.mdpi.com/2079-6374/10/10/133/htm

37. Wang C, Liu M, Wang Z, Li S, Deng Y, He N. Point-of-care diagnostics for infectious diseases: From methods to devices. Nano Today. 2021 Apr 1;37:101092.

38. Nayak S, Blumenfeld NR, Laksanasopin T, Sia SK. Point-of-Care Diagnostics: Recent Developments in a Connected Age. Anal Chem [Internet]. 2017 Jan 3 [cited 2022 May 20];89(1):102–23. Available from: https://pubs.acs.org/doi/full/10.1021/acs.analchem.6b04630

39. Meagher RJ, Hatch A V., Renzi RF, Singh AK. An integrated microfluidic platform for sensitive and rapid detection of biological toxins. Lab Chip [Internet]. 2008 [cited 2022 May 20];8(12):2046–53. Available from: https://pubmed.ncbi.nlm.nih.gov/19023467/

40. Wang H, Yang L, Chu S, Liu B, Zhang Q, Zou L, et al. Semiquantitative Visual Detection of Lead Ions with a Smartphone via a Colorimetric Paper-Based Analytical Device. Anal Chem [Internet]. 2019 Jun 20 [cited 2022 May 20];91(14):9292–9. Available from: https://pubs.acs.org/doi/full/10.1021/acs.analchem.9b02297

41. Gubala V, Harris LF, Ricco AJ, Tan MX, Williams DE. Point of care diagnostics: Status and future. Anal Chem [Internet]. 2012 Jan 17 [cited 2022 May 20];84(2):487–515. Available from: https://pubs.acs.org/doi/full/10.1021/ac2030199

42. Wu J, Kodzius R, Cao W, Wen W. Extraction, amplification and detection of DNA in microfluidic chip-based assays. Microchim Acta [Internet]. 2014 Aug 1 [cited 2022 May 20];181(13–14):1611–31. Available from: https://link.springer.com/article/10.1007/s00604-013-1140-2

43. Lagally ET, Medintz I, Mathies RA. Single-molecule DNA amplification and analysis in an integrated microfluidic device. Anal Chem [Internet]. 2001 Feb 1 [cited 2022 May 20];73(3):565–70. Available from: https://pubs.acs.org/doi/full/10.1021/ac001026b

44. Chin CD, Laksanasopin T, Cheung YK, Steinmiller D, Linder V, Parsa H, et al. Microfluidics-based diagnostics of infectious diseases in the developing world. Nat Med 2011 178 [Internet]. 2011 Jul 31 [cited 2022 May 20];17(8):1015–9. Available from: https://www.nature.com/articles/nm.2408

45. Gous N, Boeras DI, Cheng B, Takle J, Cunningham B, Peeling RW. The impact of digital technologies on point-of-care diagnostics in resource-limited settings. https://doi.org/101080/1473715920181460205 [Internet]. 2018 Apr 3 [cited 2022 May 20];18(4):385–97. Available from: https://www.tandfonline.com/doi/abs/10.1080/14737159.2018.1460205

46. Xiang Y, Lu Y. Using personal glucose meters and functional DNA sensors to quantify a variety of analytical targets. Nat Chem 2011 39 [Internet]. 2011 Jul 24 [cited 2022 May 20];3(9):697–703. Available from: https://www.nature.com/articles/nchem.1092

47. Qi L, Yang M, Chang D, Zhao W, Zhang S, Du Y, et al. A DNA Nanoflower-Assisted Separation-Free Nucleic Acid Detection Platform with a Commercial Pregnancy Test Strip. Angew Chemie Int Ed [Internet]. 2021 Nov 15 [cited 2022 May 20];60(47):24823–7. Available from: https://onlinelibrary.wiley.com/doi/full/10.1002/anie.202108827

48. Peeling RW, Olliaro PL, Boeras DI, Fongwen N. Scaling up COVID-19 rapid antigen tests: promises and challenges. Lancet Infect Dis. 2021 Sep 1;21(9):e290–5.

49. Pliakos EE, Andreatos N, Shehadeh F, Ziakas PD, Mylonakis E. The cost-effectiveness of rapid diagnostic testing for the diagnosis of bloodstream infections with or without antimicrobial stewardship. Clin Microbiol Rev [Internet]. 2018 Jul 1 [cited 2022 May 20];31(3). Available from: https://journals.asm.org/doi/full/10.1128/CMR.00095-17

50. Tao Y, Shen H, Deng K, Zhang H, Yang C. Microfluidic devices with simplified signal readout. Sensors Actuators B Chem. 2021 Jul 15;339:129730.

51. Petrusha OA, Faizuloev EB. [Detection methods for results of a loop-mediated isothermal amplification of DNA.]. Klin Lab Diagn [Internet]. 2020 Jan 1 [cited 2022 May 20];65(1):67–72. Available from: https://europepmc.org/article/med/32155010

52. Adetunji AI, Olaniran AO. Production strategies and biotechnological relevance of microbial lipases: a review. Brazilian J Microbiol [Internet]. 2021 Sep 1 [cited 2022 May 20];52(3):1257–69. Available from: https://link.springer.com/article/10.1007/s42770-021-00503-5

53. Hua Z, Yu T, Liu D, Xianyu Y. Recent advances in gold nanoparticles-based biosensors for food safety detection. Biosens Bioelectron. 2021 May 1;179:113076.

54. Jazayeri MH, Aghaie T, Avan A, Vatankhah A, Ghaffari MRS. Colorimetric detection based on gold nano particles (GNPs): An easy, fast, inexpensive, low-cost and short time

method in detection of analytes (protein, DNA, and ion). Sens Bio-Sensing Res. 2018 Sep 1;20:1–8.

55. Choi Y, Hwang JH, Lee SY. Recent Trends in Nanomaterials-Based Colorimetric Detection of Pathogenic Bacteria and Viruses. Small Methods [Internet]. 2018 Apr 1 [cited 2022 May 20];2(4):1700351. Available from: https://onlinelibrary.wiley.com/doi/full/10.1002/smtd.201700351

56. Chen J, Jackson AA, Rotello VM, Nugen SR. Colorimetric Detection of Escherichia coli Based on the Enzyme-Induced Metallization of Gold Nanorods. Small [Internet]. 2016 May 1 [cited 2022 May 20];12(18):2469–75. Available from: https://onlinelibrary.wiley.com/doi/full/10.1002/smll.201503682

57. Zeng J, Zhang Y, Zeng T, Aleisa R, Qiu Z, Chen Y, et al. Anisotropic plasmonic nanostructures for colorimetric sensing. Nano Today. 2020 Jun 1;32:100855.

58. Zorić I, Zäch M, Kasemo B, Langhammer C. Gold, platinum, and aluminum nanodisk plasmons: Material independence, subradiance, and damping mechanisms. ACS Nano [Internet]. 2011 Apr 26 [cited 2022 May 21];5(4):2535–46. Available from: https://pubs.acs.org/doi/full/10.1021/nn102166t

59. Yoon SJ, Nam YS, Lee JY, Kim JY, Lee Y, Lee KB. Highly sensitive colorimetric determination of nitrite based on the selective etching of concave gold nanocubes. Microchim Acta [Internet]. 2021 Apr 1 [cited 2022 May 21];188(4):1–11. Available from: https://link.springer.com/article/10.1007/s00604-021-04772-7

60. Csáki A, Stranik O, Fritzsche W. Localized surface plasmon resonance based biosensing. https://doi.org/101080/1473715920181440208 [Internet]. 2018 Mar 4 [cited 2022 May 21];18(3):279–96. Available from: https://www.tandfonline.com/doi/abs/10.1080/14737159.2018.1440208

61. Zhang Z, Wang H, Chen Z, Wang X, Choo J, Chen L. Plasmonic colorimetric sensors based on etching and growth of noble metal nanoparticles: Strategies and applications. Biosens Bioelectron. 2018 Aug 30;114:52–65.

62. Garibyan L, Avashia N. Polymerase chain reaction. J Invest Dermatol [Internet]. 2013 [cited 2021 Feb 28];133(3):1–4. Available from: /pmc/articles/PMC4102308/

63. Dominguez SR, Pretty K, Hengartner R, Robinson CC. Comparison of herpes simplex virus PCR with culture for virus detection in multisource surface swab specimens from neonates. J Clin Microbiol [Internet]. 2018 Oct 1 [cited 2021 Mar 10];56(10). Available from: /pmc/articles/PMC6156304/

64. Oblath EA, Henley WH, Alarie JP, Ramsey JM. A microfluidic chip integrating DNA extraction and real-time PCR for the detection of bacteria in saliva. Lab Chip [Internet]. 2013 Apr 7 [cited 2021 Feb 28];13(7):1325–32. Available from: https://pubs.rsc.org/en/content/articlehtml/2013/lc/c3lc40961a

65. Fang Y-L, Wang C-H, Chen Y-S, Chien C-C, Kuo F-C, You H-L, et al. An integrated

microfluidic system for early detection of sepsis-inducing bacteria. Lab Chip [Internet]. 2021 Jan 5 [cited 2021 Jan 13];21(1):113–21. Available from: https://pubs.rsc.org/en/content/articlehtml/2021/lc/d0lc00966k

66. Gorgannezhad L, Stratton H, Nguyen NT. Microfluidic-based nucleic acid amplification systems in microbiology [Internet]. Vol. 10, Micromachines. MDPI AG; 2019 [cited 2021 Feb 14]. Available from: /pmc/articles/PMC6630468/

67. Lakshmi BA, Kim S. Recent trends in the utilization of LAMP for the diagnosis of viruses, bacteria, and allergens in food. In: Recent Developments in Applied Microbiology and Biochemistry. Elsevier; 2021. p. 291–7.

68. Zhang H, Xu Y, Fohlerova Z, Chang H, Iliescu C, Neuzil P. LAMP-on-a-chip: Revising microfluidic platforms for loop-mediated DNA amplification. Vol. 113, TrAC - Trends in Analytical Chemistry. Elsevier B.V.; 2019. p. 44–53.

69. Li Y, Fan P, Zhou S, Zhang L. Loop-mediated isothermal amplification (LAMP): A novel rapid detection platform for pathogens. Vol. 107, Microbial Pathogenesis. Academic Press; 2017. p. 54–61.

70. Notomi T, Okayama H, Masubuchi H, Yonekawa T, Watanabe K, Amino N, et al. Loop-mediated isothermal amplification of DNA. Nucleic Acids Res [Internet]. 2000 Jun 15 [cited 2021 Feb 14];28(12):63. Available from: https://academic.oup.com/nar/article/28/12/e63/2359194

71. Shang Y, Sun J, Ye Y, Zhang J, Zhang Y, Sun X. Loop-mediated isothermal amplification-based microfluidic chip for pathogen detection [Internet]. Vol. 60, Critical Reviews in Food Science and Nutrition. Taylor and Francis Inc.; 2020 [cited 2021 Feb 14]. p. 201–24. Available from: https://www.tandfonline.com/doi/abs/10.1080/10408398.2018.1518897

72. Song J, Mauk MG, Hackett BA, Cherry S, Bau HH, Liu C. Instrument-Free Point-of-Care Molecular Detection of Zika Virus. Anal Chem [Internet]. 2016 Jul 19 [cited 2021 Feb 14];88(14):7289–94. Available from: https://pubs.acs.org/sharingguidelines

73. Ganguli A, Mostafa A, Berger J, Aydin MY, Sun F, Stewart de Ramirez SA, et al. Rapid isothermal amplification and portable detection system for SARS-CoV-2. Proc Natl Acad Sci U S A [Internet]. 2020 Sep 15 [cited 2021 Feb 14];117(37):22727–35. Available from: www.pnas.org/cgi/doi/10.1073/pnas.2014739117

74. Sun F, Ganguli A, Nguyen J, Brisbin R, Shanmugam K, Hirschberg DL, et al. Smartphone-based multiplex 30-minute nucleic acid test of live virus from nasal swab extract. Lab Chip [Internet]. 2020 May 7 [cited 2021 Feb 14];20(9):1621–7. Available from: https://pubs.rsc.org/en/content/articlehtml/2020/lc/d0lc00304b

75. Azizi M, Zaferani M, Cheong SH, Abbaspourrad A. Pathogenic Bacteria Detection Using RNA-Based Loop-Mediated Isothermal-Amplification-Assisted Nucleic Acid Amplification via Droplet Microfluidics. ACS Sensors [Internet]. 2019 Apr 26 [cited 2021 Jan 12];4(4):841–8. Available from: https://pubs.acs.org/sharingguidelines

76. Seok Y, Joung H-A, Byun J-Y, Jeon H-S, Shin SJ, Kim S, et al. A Paper-Based Device for Performing Loop-Mediated Isothermal Amplification with Real-Time Simultaneous Detection of Multiple DNA Targets. Theranostics [Internet]. 2017 [cited 2021 Jan 12];7(8):2220–30. Available from: http://www.thno.org

77. Xia Y, Guo XG, Zhou S. Rapid detection of Streptococcus pneumoniae by real-time fluorescence loop-mediated isothermal amplification. J Thorac Dis [Internet]. 2014 [cited 2021 Feb 28];6(9):1193–9. Available from: /pmc/articles/PMC4178110/

78. Seo JH, Park BH, Oh SJ, Choi G, Kim DH, Lee EY, et al. Development of a high-throughput centrifugal loop-mediated isothermal amplification microdevice for multiplex foodborne pathogenic bacteria detection. Sensors Actuators, B Chem. 2017 Jul 1;246:146–53.

79. Zhang L, Tian F, Liu C, Feng Q, Ma T, Zhao Z, et al. Hand-powered centrifugal microfluidic platform inspired by the spinning top for sample-to-answer diagnostics of nucleic acids. Lab Chip [Internet]. 2018 Feb 21 [cited 2021 Jan 13];18(4):610–9. Available from: https://pubs.rsc.org/en/content/articlehtml/2018/lc/c7lc01234a

80. Yuan H, Chao Y, Shum HC. Droplet and Microchamber-Based Digital Loop-Mediated Isothermal Amplification (dLAMP). Small [Internet]. 2020 Mar 3 [cited 2021 Feb 28];16(9):1904469. Available from: https://onlinelibrary.wiley.com/doi/abs/10.1002/smll.201904469

81. Ma YD, Luo K, Chang WH, Lee G Bin. A microfluidic chip capable of generating and trapping emulsion droplets for digital loop-mediated isothermal amplification analysis. Lab Chip [Internet]. 2018 Jan 21 [cited 2021 Feb 28];18(2):296–303. Available from: https://pubs.rsc.org/en/content/articlehtml/2018/lc/c7lc01004d

82. Kim HJ, Kim YJ, Yong DE, Lee K, Park JH, Lee JM, et al. Loop-mediated isothermal amplification of vanA gene enables a rapid and naked-eye detection of vancomycin-resistant enterococci infection. J Microbiol Methods. 2014 Sep 1;104:61–6.

83. Zhang Z, Zhao S, Hu F, Yang G, Li J, Tian H, et al. An LED-Driven AuNPs-PDMS Microfluidic Chip and Integrated Device for the Detection of Digital Loop-Mediated Isothermal DNA Amplification. Micromachines [Internet]. 2020 Feb 8 [cited 2021 Feb 28];11(2):177. Available from: https://www.mdpi.com/2072-666X/11/2/177

84. Aydin S. A short history, principles, and types of ELISA, and our laboratory experience with peptide/protein analyses using ELISA. Peptides. 2015 Mar 13;72:4–15.

85. Alhajj M, Farhana A. Enzyme Linked Immunosorbent Assay [Internet]. StatPearls. StatPearls Publishing; 2020 [cited 2021 Feb 22]. Available from: http://www.ncbi.nlm.nih.gov/pubmed/32310382

86. Khatkhatay MI, Desai M. A comparison of performances of four enzymes used in ELISA with special reference to β-lactamase. J Immunoassay. 1999;20(3):151–83.

87. Bass JJ, Wilkinson DJ, Rankin D, Phillips BE, Szewczyk NJ, Smith K, et al. An overview

of technical considerations for Western blotting applications to physiological research. Vol. 27, Scandinavian Journal of Medicine and Science in Sports. Blackwell Munksgaard; 2017. p. 4–25.

88. Wu JH, Wang CH, Ma YD, Lee G Bin. A nitrocellulose membrane-based integrated microfluidic system for bacterial detection utilizing magnetic-composite membrane microdevices and bacteria-specific aptamers. Lab Chip [Internet]. 2018 Jun 7 [cited 2021 Jan 14];18(11):1633–40. Available from: https://pubs.rsc.org/en/content/articlehtml/2018/lc/c8lc00251g

89. Zheng L, Cai G, Wang S, Liao M, Li Y, Lin J. A microfluidic colorimetric biosensor for rapid detection of Escherichia coli O157:H7 using gold nanoparticle aggregation and smart phone imaging. Biosens Bioelectron. 2019 Jan 15;124–125:143–9.

90. Melendez JH, Frankel YM, An AT, Williams L, Price LB, Wang NY, et al. Real-time PCR assays compared to culture-based approaches for identification of aerobic bacteria in chronic wounds. Clin Microbiol Infect. 2010 Dec 1;16(12):1762–9.

91. Alhajj M, Farhana A. Enzyme Linked Immunosorbent Assay [Internet]. StatPearls. StatPearls Publishing; 2021 [cited 2021 Mar 3]. Available from: http://www.ncbi.nlm.nih.gov/pubmed/32310382

92. Doron S, Gorbach SL. Bacterial infections: Overview. In: International Encyclopedia of Public Health [Internet]. Elsevier Inc.; 2008 [cited 2021 Mar 18]. p. 273–82. Available from: /pmc/articles/PMC7149789/

93. Environmental Protection Agency U. Approved CWA Microbiological Test Methods. [cited 2021 Mar 18]; Available from: https://www.epa.gov/cwa-methods/approved-cwa-microbiological-test-methods

94. Chen P, Chen C, Su H, Zhou M, Li S, Du W, et al. Integrated and finger-actuated microfluidic chip for point-of-care testing of multiple pathogens. Talanta. 2021 Mar 1;224:121844.

95. Wang S, Liu N, Zheng L, Cai G, Lin J. A lab-on-chip device for the sample-in-result-out detection of viable: Salmonella using loop-mediated isothermal amplification and real-time turbidity monitoring. Lab Chip [Internet]. 2020 Jul 7 [cited 2021 Jan 15];20(13):2296–305. Available from: https://pubs.rsc.org/en/content/articlehtml/2020/lc/d0lc00290a

96. Liu D, Zhu Y, Li N, Lu Y, Cheng J, Xu Y. A portable microfluidic analyzer for integrated bacterial detection using visible loop-mediated amplification. Sensors Actuators, B Chem. 2020 May 1;310:127834.

97. Nguyen H Van, Nguyen VD, Lee EY, Seo TS. Point-of-care genetic analysis for multiplex pathogenic bacteria on a fully integrated centrifugal microdevice with a large-volume sample. Biosens Bioelectron. 2019 Jul 1;136:132–9.

98. Trinh KTL, Trinh TND, Lee NY. Fully integrated and slidable paper-embedded plastic

microdevice for point-of-care testing of multiple foodborne pathogens. Biosens Bioelectron. 2019 Jun 15;135:120–8.

99. Sayad A, Ibrahim F, Mukim Uddin S, Cho J, Madou M, Thong KL. A microdevice for rapid, monoplex and colorimetric detection of foodborne pathogens using a centrifugal microfluidic platform. Biosens Bioelectron. 2018 Feb 15;100:96–104.

100. Pang B, Fu K, Liu Y, Ding X, Hu J, Wu W, et al. Development of a self-priming PDMS/paper hybrid microfluidic chip using mixed-dye-loaded loop-mediated isothermal amplification assay for multiplex foodborne pathogens detection. Anal Chim Acta. 2018 Dec 21;1040:81–9.

101. Ma YD, Luo K, Chang WH, Lee G Bin. A microfluidic chip capable of generating and trapping emulsion droplets for digital loop-mediated isothermal amplification analysis. Lab Chip [Internet]. 2018 Jan 21 [cited 2021 Feb 14];18(2):296–303. Available from: https://pubs.rsc.org/en/content/articlehtml/2018/lc/c7lc01004d

102. Chen SL, Chang WH, Wang CH, You HL, Wu JJ, Liu TH, et al. An integrated microfluidic system for live bacteria detection from human joint fluid samples by using ethidium monoazide and loop-mediated isothermal amplification. Microfluid Nanofluidics [Internet]. 2017 May 1 [cited 2021 Feb 18];21(5):87. Available from: https://link.springer.com/article/10.1007/s10404-017-1913-8

103. Chen C, Liu P, Zhao X, Du W, Feng X, Liu BF. A self-contained microfluidic in-gel loop-mediated isothermal amplification for multiplexed pathogen detection. Sensors Actuators, B Chem. 2017 Feb 1;239:1–8.

104. Dou M, Sanjay ST, Dominguez DC, Liu P, Xu F, Li XJ. Multiplexed instrument-free meningitis diagnosis on a polymer/paper hybrid microfluidic biochip. Biosens Bioelectron. 2017 Jan 15;87:865–73.

105. Oh SJ, Park BH, Jung JH, Choi G, Lee DC, Kim DH, et al. Centrifugal loop-mediated isothermal amplification microdevice for rapid, multiplex and colorimetric foodborne pathogen detection. Biosens Bioelectron. 2016 Jan 15;75:293–300.

106. Oh SJ, Park BH, Choi G, Seo JH, Jung JH, Choi JS, et al. Fully automated and colorimetric foodborne pathogen detection on an integrated centrifugal microfluidic device. Lab Chip [Internet]. 2016 May 10 [cited 2021 Jan 14];16(10):1917–26. Available from: www.rsc.org/loc

107. Sayad AA, Ibrahim F, Uddin SM, Pei KX, Mohktar MS, Madou M, et al. A microfluidic lab-on-a-disc integrated loop mediated isothermal amplification for foodborne pathogen detection. Sensors Actuators, B Chem. 2016 May 1;227:600–9.

108. Dey P, Fabri-Faja N, Calvo-Lozano O, Terborg RA, Belushkin A, Yesilkoy F, et al. Label-free Bacteria Quantification in Blood Plasma by a Bioprinted Microarray Based Interferometric Point-of-Care Device. ACS Sensors [Internet]. 2019 Jan 25 [cited 2021 Jan 11];4(1):52–60. Available from: http://www.rais-project.eu/

109. Wang CH, Wu JJ, Lee G Bin. Screening of highly-specific aptamers and their applications in paper-based microfluidic chips for rapid diagnosis of multiple bacteria. Sensors Actuators, B Chem. 2019 Apr 1;284:395–402.

110. Wang C, Gao X, Wang S, Liu Y. A smartphone-integrated paper sensing system for fluorescent and colorimetric dual-channel detection of foodborne pathogenic bacteria. Anal Bioanal Chem [Internet]. 2020 Jan 1 [cited 2021 Jan 12];412(3):611–20. Available from: https://doi.org/10.1007/s00216-019-02208-z

111. Hossein-Nejad-Ariani H, Kim T, Kaur K. Peptide-Based Biosensor Utilizing Fluorescent Gold Nanoclusters for Detection of Listeria monocytogenes. ACS Appl Nano Mater [Internet]. 2018 Jul 27 [cited 2021 Jan 12];1(7):3389–97. Available from: https://pubs.acs.org/sharingguidelines

112. Erdem T, Demir HV. Light stimulus and human eye. SpringerBriefs Appl Sci Technol Nanosci Nanotechnol [Internet]. 2019 [cited 2022 Jun 17];5–9. Available from: https://link.springer.com/chapter/10.1007/978-981-13-5886-9_2

113. Etxabide A, Kilmartin PA, Maté JI. Color stability and pH-indicator ability of curcumin, anthocyanin and betanin containing colorants under different storage conditions for intelligent packaging development. Food Control. 2021 Mar 1;121:107645.

114. Špačková B, Wrobel P, Bocková M, Homola J. Optical Biosensors Based on Plasmonic Nanostructures: A Review. Proc IEEE. 2016 Dec 1;104(12):2380–408.